CHAPTER 6

RADIATIVE EXCHANGE BETWEEN PARTIALLY SPECULAR GRAY SURFACES

6.1 INTRODUCTION

In the previous two chapters it was assumed that all surfaces constituting the enclosure are—besides being gray—diffuse emitters as well as diffuse reflectors of radiant energy. Diffuse emission is nearly always an acceptable simplification. The assumption of diffuse reflection, on the other hand, often leads to considerable error, since many surfaces deviate substantially from this behavior. Electromagnetic wave theory predicts reflection to be specular for optically smooth surfaces, i.e., to reflect light like a mirror. All clean metals, many nonmetals such as glassy materials, and most polished materials display strong specular reflection peaks. Nevertheless, they all, to some extent, reflect somewhat into other directions as a result of their surface roughness. Surfaces may appear dull (i.e., diffusely reflecting) to the eye, but are rather specular in the infrared, since the ratio of every surface's root-mean-square roughness to wavelength decreases with increasing wavelength.

For a surface with diffuse reflectance the reflected radiation has the same (diffuse) directional distribution as the emitted energy, as discussed in the beginning of Section 5.3. Therefore, the radiation field within the enclosure is completely specified in terms of the radiosity, which is a function of location along the enclosure walls (but *not* a function of *direction* as well). If reflection is nondiffuse, then the radiation intensities leaving any surface are functions of direction as well as surface location, and the analysis becomes immensely more complicated.[1] To make the analysis tractable, one may make the idealization that the reflectance, while not diffuse, can be adequately represented by a combination of a diffuse and a specular component, as illustrated in Fig. 6-1 for oxidized brass [1]. Thus, for the present chapter, we assume the radiative properties to be of the form

$$\rho = \rho^s + \rho^d = 1 - \alpha = 1 - \epsilon = 1 - \epsilon'_\lambda, \tag{6.1}$$

where ρ^s and ρ^d are the specular and diffuse components of the reflectance, respectively. Since the surfaces are assumed to be gray, diffuse emitters ($\epsilon = \epsilon'_\lambda$), it follows that neither α nor ρ

[1] In addition, if the irradiation is polarized (e.g., owing to irradiation from a laser source), specular reflections will change the state of polarization (because of the different values for $\rho_\parallel$ and $\rho_\perp$, as discussed in Chapter 2). We shall only consider unpolarized radiation.

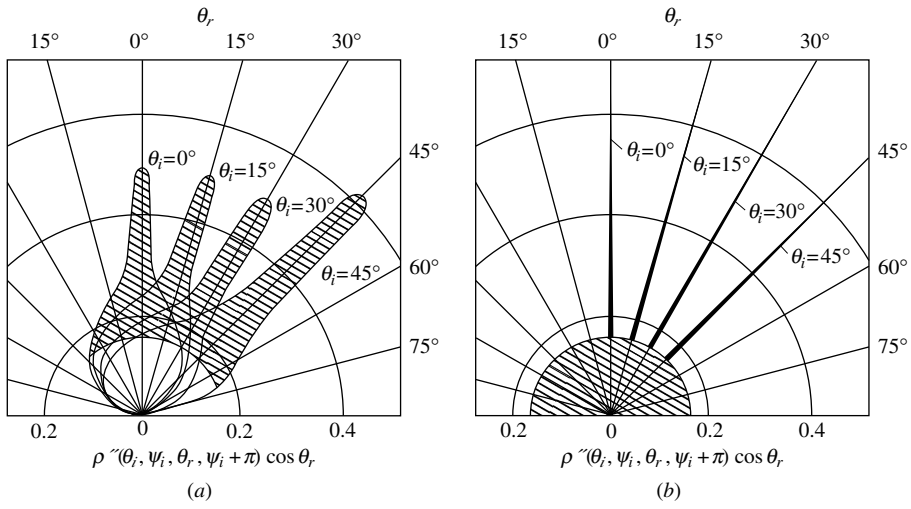

FIGURE 6-1
(*a*) Subdivision of the reflectance of oxidized brass (shown for plane of incidence) into specular (shaded) and diffuse components (unshaded), from [1]; (*b*) equivalent idealized reflectance.

may depend on wavelength or on *incoming* direction (i.e., the *magnitude* of ρ does not depend on incoming direction); how ρ is distributed over *outgoing* directions depends on incoming direction through ρ^s. With this approximation, the separate reflection components may be found analytically by splitting the bidirectional reflection function into two parts,

$$\rho''(\mathbf{r}, \hat{\mathbf{s}}_i, \hat{\mathbf{s}}_r) = \rho''^s(\mathbf{r}, \hat{\mathbf{s}}_i, \hat{\mathbf{s}}_r) + \rho''^d(\mathbf{r}, \hat{\mathbf{s}}_i, \hat{\mathbf{s}}_r). \tag{6.2}$$

Substituting this expression into equation (3.43) and equation (3.46) then leads to ρ^s and ρ^d. Values of ρ^s and ρ^d may also be determined directly from experiment, as reported by Birkebak and coworkers [2], making detailed measurements of the bidirectional reflection function unnecessary.

Within an enclosure consisting of surfaces with purely diffuse and purely specular reflection components, the complexity of the problem may be reduced considerably by realizing that any specularly reflected beam may be traced back to a point on the enclosure surface from which it emanated diffusely (i.e., any beam was part of an energy stream leaving the surface after emission or diffuse reflection), as illustrated in Fig. 6-2. Therefore, by redefining the view factors to include specular reflection paths in addition to direct view, the radiation field may again be described by a diffuse energy function that is a function of surface location but not of direction.

6.2 SPECULAR VIEW FACTORS

To accommodate surfaces with reflectances described by equation (6.1), we define a *specular view factor* as

$$dF^s_{dA_i - dA_j} \equiv \frac{\begin{array}{c}\text{diffuse energy leaving } dA_i \text{ intercepted by } dA_j, \text{ by} \\ \text{direct travel or any number of specular reflections}\end{array}}{\text{total diffuse energy leaving } dA_i}. \tag{6.3}$$

The concept of the specular view factor is illustrated in Figs. 6-2 and 6-3. Diffuse radiation leaving dA_i (by emission or diffuse reflection) can reach dA_j either directly or after one or more reflections. Usually only a finite number of specular reflection paths such as $dA_i - a - dA_j$ or $dA_i - b - c - dA_j$ (and others not indicated in the figure) will be possible. The surface at points

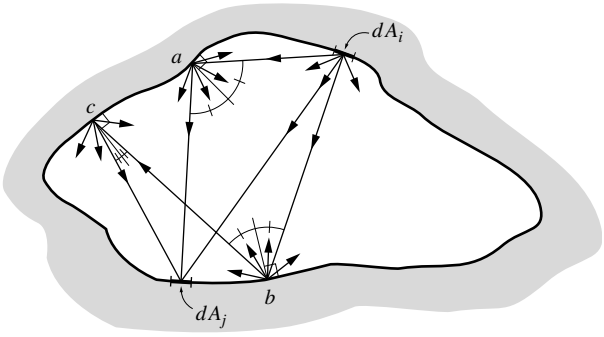

FIGURE 6-2
Radiative exchange in an enclosure with specular reflectors.

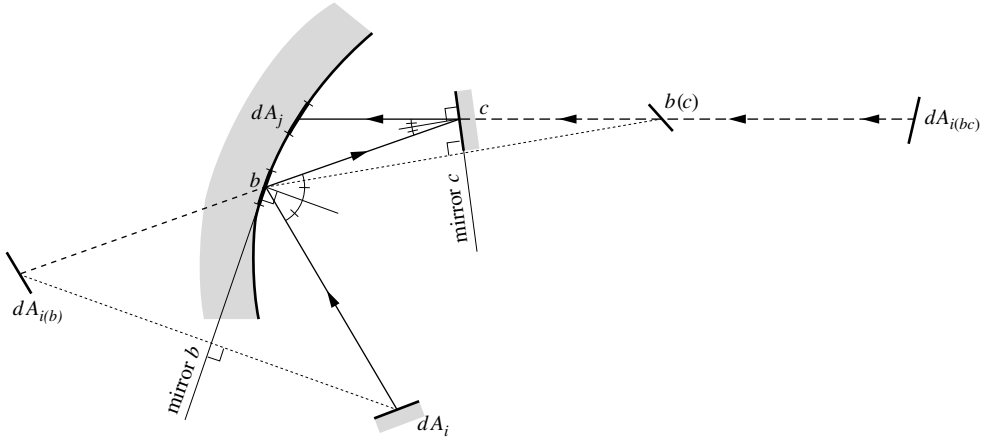

FIGURE 6-3
Specular view factor between infinitesimal surface elements; formation of images.

a, *b*, and *c* behaves like a perfect mirror as far as the specular part of the reflection is concerned. Therefore, if an observer stood on top of dA_j looking toward *c*, it would appear as if point *b* as well as dA_i were situated *behind* point *c* as indicated in Fig. 6-3; the point labeled *b*(*c*) is the *image* of point *b* as *mirrored* by the surface at *c*, and $dA_i(cb)$ is the image of dA_i as mirrored by the surfaces at *c* and *b*. Therefore, as we examine Figs. 6-2 and 6-3, we may formally evaluate the specular view factor between two infinitesimal areas as

$$dF^s_{dA_i-dA_j} = dF_{dA_i-dA_j} + \rho^s_a\, dF_{dA_i(a)-dA_j} + \rho^s_b\rho^s_c\, dF_{dA_i(cb)-dA_j} + \text{other possible reflection paths.} \tag{6.4}$$

Thus, the specular view factor may be expressed as a sum of diffuse view factors, with one contribution for each possible direct or reflection path. Note that, for images, the diffuse view factors must be multiplied by the specular reflectances of the mirroring surfaces, since radiation traveling from dA_i to dA_j is attenuated by every reflection.

If all specularly reflecting parts of the enclosure are flat, then all images of dA_i have the same shape and size as dA_i itself. However, curved surfaces tend to distort the images (focusing and defocusing effects). In the case of only flat, specularly reflecting surfaces we may multiply equation (6.4) by dA_i and, invoking the law of reciprocity for diffuse view factors, equation (4.7), we obtain

$$\begin{aligned} dA_i\, dF^s_{dA_i-dA_j} &= dA_j\, dF_{dA_j-dA_i} + \rho^s_a\, dA_j\, dF_{dA_j-dA_i(a)} + \rho^s_b\rho^s_c\, dA_j\, dF_{dA_j-dA_i(bc)} \\ &= dA_j\, dF_{dA_j-dA_i} + \rho^s_a\, dA_j\, dF_{dA_j(a)-dA_i} + \rho^s_b\rho^s_c\, dA_j\, dF_{dA_j(bc)-dA_i} + \dots \\ &= dA_j\, dF^s_{dA_j-dA_i}, \end{aligned} \tag{6.5}$$

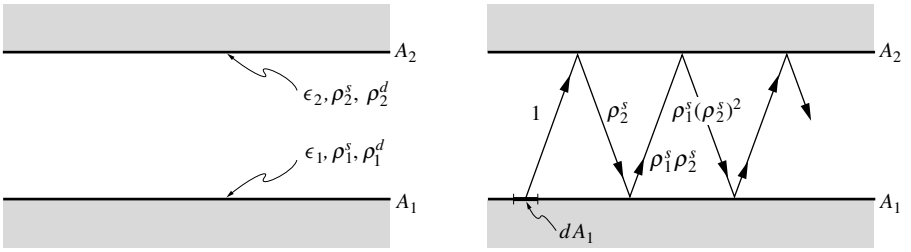

FIGURE 6-4
(*a*) Geometry for Example 6.1, (*b*) ray tracing for the evaluation of F^s_{1-1} and F^s_{1-2}.

that is, the *law of reciprocity* holds for specular view factors as long as all specularly reflecting surfaces are flat. Although considerably more complicated, it is possible to show that the law of reciprocity also holds for curved specular reflectors. If we also assume that the diffuse energy leaving A_i and A_j is constant across each respective area, we have the equivalent to equation (4.15),

$$dA_i\, dF^s_{di-dj} = dA_j\, dF^s_{dj-di}, \tag{6.6a}$$

$$dA_i\, F^s_{di-j} = A_j\, dF^s_{j-di}, \qquad (J_j = \text{const}), \tag{6.6b}$$

$$A_i\, F^s_{i-j} = A_j\, F^s_{j-i}, \qquad (J_i,\ J_j = \text{const}), \tag{6.6c}$$

where we have adopted the compact notation first introduced in Chapter 4, and J_i is the total diffuse energy (per unit area) leaving surface A_i (again called the *radiosity*).

Example 6.1. Evaluate the specular view factors F^s_{1-1} and F^s_{1-2} for the parallel plate geometry shown in Fig. 6-4*a*.

Solution
We note that, because of the one-dimensionality of the problem, F^s_{d1-2} must be the same for any dA_1 on surface A_1. Since F^s_{1-2} is nothing but a surface average of F^s_{d1-2}, we conclude that $F^s_{d1-2} = F^s_{1-2}$. It is sufficient to consider energy leaving from an infinitesimal area (rather than all of A_1). Examining Fig. 6-4*b* we see that every beam (assumed to have unity strength) leaving dA_1, regardless of its direction, must travel to surface A_2 (a beam of strength "1" is intercepted). After reflection at A_2 a beam of strength ρ^s_2 returns to A_1 specularly, where it is reflected again and a beam of strength $\rho^s_2\rho^s_1$ returns to A_2 specularly. After one more reflection a beam of strength $(\rho^s_2\rho^s_1)\rho^s_2$ returns to A_1, and so on. Thus, the specular view factor may be evaluated as

$$F^s_{d1-2} = F^s_{1-2} = 1 + \rho^s_1\rho^s_2 + (\rho^s_1\rho^s_2)^2 + (\rho^s_1\rho^s_2)^3 + \ldots. \tag{6.7}$$

Since $\rho^s_1\rho^s_2 < 1$ the sum in this equation is readily evaluated by the methods given in Wylie [3], and

$$F^s_{1-2} = \frac{1}{1-\rho^s_1\rho^s_2} = F^s_{2-1}. \tag{6.8}$$

The last part of this relation is found by switching subscripts or by invoking reciprocity (and $A_1 = A_2$). We notice that specular view factors are not limited to values between zero and one, but are often greater than unity because much of the radiative energy leaving a surface is accounted for more than once. All energy from A_1 is intercepted by A_2 after direct travel, but only the fraction $(1-\rho^s_2)$ is removed (by absorption and/or diffuse reflection) from the specular reflection path. The fraction ρ^s_2 travels on specularly and is, therefore, counted a second time, etc. Thus, it is $(1-\rho^s_2)F^s_{1-2}$ that must have a value between zero and one, and the *summation relation*, equation (4.18), must be replaced by

$$\sum_{j=1}^{N}(1-\rho^s_j)F^s_{i-j} = 1. \tag{6.9}$$

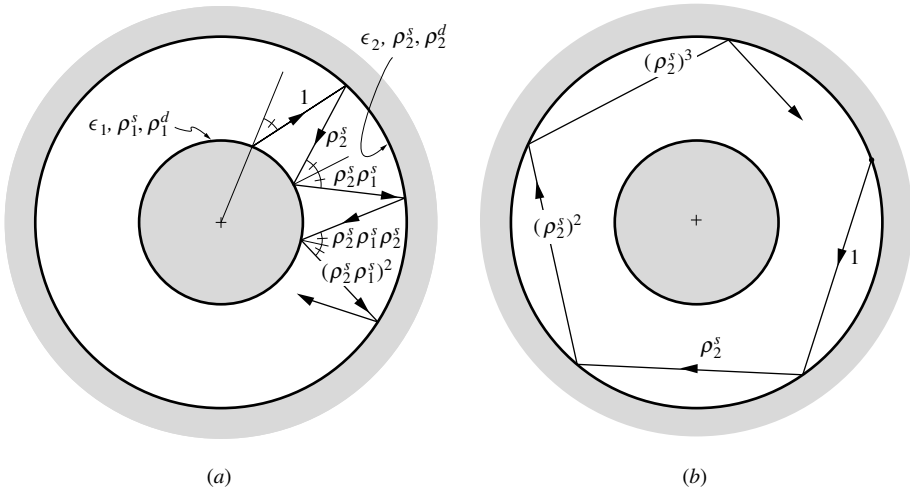

FIGURE 6-5
(*a*) Geometry for Example 6.2, (*b*) repeated reflections along outer surface.

Equation (6.9), formed here through intuition, will be developed rigorously in the next section.

F^s_{1-1} may be found similarly as

$$F^s_{1-1} = \rho^s_2 + (\rho^s_1\rho^s_2)\rho^s_2 + (\rho^s_1\rho^s_2)^2\rho^s_2 + \ldots = \frac{\rho^s_2}{1-\rho^s_1\rho^s_2}.$$

We note in passing that

$$(1-\rho^s_1)F^s_{1-1} + (1-\rho^s_2)F^s_{1-2} = \frac{(1-\rho^s_1)\rho^s_2 + 1 - \rho^s_2}{1-\rho^s_1\rho^s_2} = 1,$$

as postulated by equation (6.9).

Example 6.2. Evaluate all specular view factors for two concentric cylinders or spheres.

Solution

Possible beam paths with specular reflections from inner to outer cylinders (or spheres) and vice versa are shown in Fig. 6-5*a*. As in the previous example a beam leaving A_1 in any direction must hit surface A_2 (with strength "1"). Because of the circular geometry, after specular reflection the beam (now of strength ρ^s_2) *must* return to A_1 (i.e., it cannot hit A_2 again before hitting A_1). After renewed reflections the beam keeps bouncing back and forth between A_1 and A_2. Thus, as for parallel plates,

$$F^s_{1-2} = 1 + \rho^s_1\rho^s_2 + (\rho^s_1\rho^s_2)^2 + \ldots = \frac{1}{1-\rho^s_1\rho^s_2}.$$

Similarly, we have

$$F^s_{1-1} = \rho^s_2 + (\rho^s_1\rho^s_2)\rho^s_2 + \ldots = \frac{\rho^s_2}{1-\rho^s_1\rho^s_2}.$$

A beam emanating from A_2 will first hit either A_1, and then keep bouncing back and forth between A_1 and A_2 (cf. Fig. 6-5*a*), or A_2, and then keep bouncing along A_2 without ever hitting A_1 (cf. Fig. 6-5*b*). Thus, since the fraction F_{2-1} of the diffuse energy leaving A_2 hits A_1 after direct travel, we have

$$\begin{aligned} F^s_{2-1} &= F_{2-1}\left[1 + \rho^s_1\rho^s_2 + (\rho^s_1\rho^s_2)^2 + \ldots\right] = \frac{A_1/A_2}{1-\rho^s_1\rho^s_2}, \\ F^s_{2-2} &= F_{2-2}\left[1 + \rho^s_2 + (\rho^s_2)^2 + (\rho^s_2)^3 + \ldots\right] + F_{2-1}\left[\rho^s_1 + \rho^s_1(\rho^s_1\rho^s_2) + \ldots\right] \\ &= \frac{1 - A_1/A_2}{1-\rho^s_2} + \frac{\rho^s_1 A_1/A_2}{1-\rho^s_1\rho^s_2}, \end{aligned}$$

where the simple diffuse view factors F_{2-1} and F_{2-2} have been evaluated in terms of A_1 and A_2. Of course, F^s_{2-1} could have been found from F^s_{1-2} by reciprocity, and F^s_{2-2} with the aid of equation (6.9).

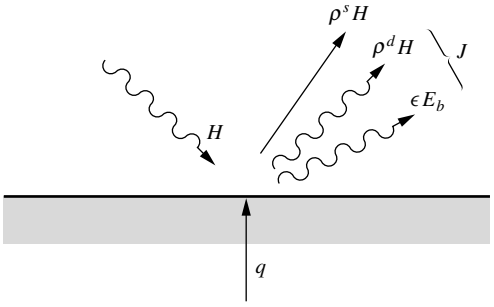

FIGURE 6-6
Energy balance for surfaces with partially specular reflection.

A few more examples of specular view factor determinations will be given once the appropriate heat transfer relations have been developed.

6.3 ENCLOSURES WITH PARTIALLY SPECULAR SURFACES

Consider an enclosure of arbitrary geometry as shown in Fig. 6-2. All surfaces are gray, diffuse emitters and gray reflectors with purely diffuse and purely specular components, i.e., their radiative properties obey equation (6.1). Under these conditions the net heat flux at a surface at location **r** is, from Fig. 6-6,

$$\begin{aligned} q(\mathbf{r}) &= q_{\text{emission}} - q_{\text{absorption}} = \epsilon(\mathbf{r})[E_b(\mathbf{r}) - H(\mathbf{r})] \\ &= q_{\text{out}} - q_{\text{in}} = \epsilon(\mathbf{r})E_b(\mathbf{r}) + \rho^d(\mathbf{r})H(\mathbf{r}) + \rho^s(\mathbf{r})H(\mathbf{r}) - H(\mathbf{r}). \end{aligned} \tag{6.10}$$

The first two terms on the last right-hand side of equation (6.10), or the part of the outgoing heat flux that leaves diffusely, we will again call the *surface radiosity*,

$$J(\mathbf{r}) = \epsilon(\mathbf{r})E_b(\mathbf{r}) + \rho^d(\mathbf{r})H(\mathbf{r}), \tag{6.11}$$

so that

$$q(\mathbf{r}) = J(\mathbf{r}) - [1 - \rho^s(\mathbf{r})]H(\mathbf{r}). \tag{6.12}$$

Eliminating the irradiation $H(\mathbf{r})$ from equations (6.10) and (6.12) leads to

$$q(\mathbf{r}) = \frac{\epsilon(\mathbf{r})}{\rho^d(\mathbf{r})}\Big[[1 - \rho^s(\mathbf{r})]E_b(\mathbf{r}) - J(\mathbf{r})\Big], \tag{6.13}$$

which, of course, reduces to equation (5.26) for a diffusely reflecting surface if $\rho^s = 0$ and $\rho^d = 1 - \epsilon$. For a purely specular reflecting surface ($\rho^d = 0$) equation (6.13) is indeterminate since the radiosity consists only of emission, or $J = \epsilon E_b$.

As in Chapter 5 the irradiation $H(\mathbf{r})$ is found by determining the contribution to H from a differential area $dA'(\mathbf{r}')$, followed by integration over the entire enclosure surface. A subtle difference is that we do not track the total energy leaving dA' (multiplied by a suitable direct-travel view factor); rather, the contribution from specular reflections is subtracted and attributed to the surface from which it leaves diffusely. The more complicated path of such energy is then accounted for by the definition of the specular view factor. Thus, similar to equation (5.21),

$$H(\mathbf{r})\,dA = \int_A J(\mathbf{r}')\,dF^s_{dA'-dA}\,dA' + H^s_o(\mathbf{r})\,dA, \tag{6.14}$$

where $H^s_o(\mathbf{r})$ is any external irradiation arriving at dA (through openings or semitransparent walls). Similar to the specular view factors, the H^s_o includes external radiation hitting *dA directly*

or *after any number of specular reflections*. Using reciprocity, equation (6.14) becomes

$$H(\mathbf{r}) = \int_A J(\mathbf{r}')\, dF^s_{dA-dA'} + H^s_o(\mathbf{r}), \tag{6.15}$$

and, after substitution into equation (6.11), an integral equation for the unknown radiosity is obtained as

$$J(\mathbf{r}) = \epsilon(\mathbf{r})E_b(\mathbf{r}) + \rho^d(\mathbf{r})\left[\int_A J(\mathbf{r}')\, dF^s_{dA-dA'} + H^s_o(\mathbf{r})\right]. \tag{6.16}$$

For surface locations for which heat flux $q(\mathbf{r})$ is given rather than $E_b(\mathbf{r})$, equation (6.12) should be used rather than equation (6.11). It is usually more desirable to eliminate the radiosity, to obtain a single relationship between surface blackbody emissive powers and heat fluxes. Solving equation (6.13) for J gives

$$J(\mathbf{r}) = \left[1 - \rho^s(\mathbf{r})\right] E_b(\mathbf{r}) - \frac{\rho^d(\mathbf{r})}{\epsilon(\mathbf{r})} q(\mathbf{r}), \tag{6.17}$$

and substituting this expression into equation (6.16) leads to

$$(1-\rho^s)E_b - \frac{\rho^d}{\epsilon} q = (1-\rho^s-\rho^d)E_b + \rho^d\left[\int_A (1-\rho^s)E_b\, dF^s_{dA-dA'} - \int_A \frac{\rho^d}{\epsilon} q\, dF^s_{dA-dA'} + H^s_o\right],$$

or

$$E_b(\mathbf{r}) - \int_A \left[1 - \rho^s(\mathbf{r}')\right] E_b(\mathbf{r}')\, dF^s_{dA-dA'} = \frac{q(\mathbf{r})}{\epsilon(\mathbf{r})} - \int_A \frac{\rho^d(\mathbf{r}')}{\epsilon(\mathbf{r}')} q(\mathbf{r}')\, dF^s_{dA-dA'} + H^s_o(\mathbf{r}). \tag{6.18}$$

We note that, for diffusely reflecting surfaces with $\rho^s = 0$, $\rho^d = 1 - \epsilon$, $F^s_{i-j} = F_{i-j}$, and $H^s_o = H_o$, equation (6.18) reduces to equation (5.28). If the specular view factors can be calculated (and that is often a big "if"), then equation (6.18) is not any more difficult to solve than equation (5.28). Indeed, if part or all of the surface is purely specular ($\rho^d = 0$), equation (6.18) becomes considerably simpler.

As for black and gray-diffuse enclosures, it is customary to simplify the analysis by using an idealized enclosure, consisting of N relatively simple subsurfaces, over each of which the radiosity is assumed constant. Then

$$\int_A J(\mathbf{r}')\, dF^s_{dA-dA'} \simeq \sum_{j=1}^{N} J_j \int_{A_j} dF^s_{dA-dA_j} = \sum_{j=1}^{N} J_j\, F^s_{dA-A_j},$$

and, after averaging over a subsurface A_i on which dA is situated, equation (6.16) simplifies to

$$J_i = \epsilon_i E_{bi} + \rho^d_i \left(\sum_{j=1}^{N} J_j\, F^s_{i-j} + H^s_{oi}\right), \quad i = 1, 2, \ldots, N. \tag{6.19}$$

Eliminating radiosity through equation (6.17) then simplifies equation (6.18) to

$$E_{bi} - \sum_{j=1}^{N} (1 - \rho^s_j) F^s_{i-j} E_{bj} = \frac{q_i}{\epsilon_i} - \sum_{j=1}^{N} \frac{\rho^d_j}{\epsilon_j} F^s_{i-j} q_j + H^s_{oi}, \quad i = 1, 2, \ldots, N. \tag{6.20}$$

The *summation relation*, equation (6.9), is easily obtained from equation (6.20) by considering a special case: In an isothermal enclosure ($E_{b1} = E_{b2} = \cdots = E_{bN}$) without external irradiation

($H^s_{o1} = H^s_{o2} = \cdots = 0$), according to the Second Law of Thermodynamics, all heat fluxes must vanish ($q_1 = q_2 = \cdots = 0$). Thus, canceling emissive powers,

$$\sum_{j=1}^{N}(1-\rho^s_j)F^s_{i-j} = 1, \qquad i = 1, 2, \ldots, N. \tag{6.21}$$

Since the F^s_{i-j} are *geometric* factors and do not depend on temperature distribution, equation (6.21) is valid for arbitrary emissive power values.

Finally, for computer calculations it may be advantageous to write the emissive power and heat fluxes in matrix form. Introducing Kronecker's delta equation (6.20) becomes

$$\sum_{j=1}^{N}\left[\delta_{ij} - (1-\rho^s_j)F^s_{i-j}\right]E_{bj} = \sum_{j=1}^{N}\left(\frac{\delta_{ij}}{\epsilon_j} - \frac{\rho^d_j}{\epsilon_j}F^s_{i-j}\right)q_j + H^s_{oi}, \quad i = 1, 2, \ldots, N, \tag{6.22}$$

or[2]

$$\mathbf{A}\cdot\mathbf{e_b} = \mathbf{C}\cdot\mathbf{q} + \mathbf{h^s_o}, \tag{6.23}$$

where $\mathbf{C}$ and $\mathbf{A}$ are matrices with elements

$$\begin{aligned} A_{ij} &= \delta_{ij} - (1-\rho^s_j)F^s_{i-j}, \\ C_{ij} &= \frac{\delta_{ij}}{\epsilon_j} - \frac{\rho^d_j}{\epsilon_j}F^s_{i-j}, \end{aligned}$$

and $\mathbf{q}$, $\mathbf{e_b}$, and $\mathbf{h^s_o}$ are vectors for the surface heat fluxes, emissive powers, and external irradiations, respectively. If all temperatures and external irradiations are known, the unknown heat fluxes are readily found by matrix inversion as

$$\mathbf{q} = \mathbf{C}^{-1}\cdot\left[\mathbf{A}\cdot\mathbf{e_b} - \mathbf{h^s_o}\right]. \tag{6.24}$$

If the emissive power is only known over some of the surfaces, and the heat fluxes are specified elsewhere, equation (6.23) may be rearranged into a similar equation for the vector containing all the unknowns. Subroutine `graydifspec` is provided in Appendix F for the solution of the simultaneous equations (6.23), requiring surface information and a partial view factor matrix as input. The solution to a sample problem is also given in the form of a program `grspecxch`, which may be used as a starting point for the solution to other problems. Fortran90, C++ as well as MATLAB® versions are provided.

Example 6.3. Two large parallel plates are separated by a nonparticipating medium as shown in Fig. 6-4*a*. The bottom surface is isothermal at T_1, with emittance ϵ_1 and a partially specular, partially diffuse reflectance $\rho_1 = \rho^d_1 + \rho^s_1$. Similarly, the top surface is isothermal at T_2 with ϵ_2 and $\rho_2 = \rho^d_2 + \rho^s_2$. Determine the radiative heat flux between the surfaces.

Solution
From equation (6.20) we have, for $i = 1$, with $H^s_{o1} = 0$,

$$E_{b1} - (1-\rho^s_1)F^s_{1-1}E_{b1} - (1-\rho^s_2)F^s_{1-2}E_{b2} = \frac{q_1}{\epsilon_1} - \frac{\rho^d_1}{\epsilon_1}F^s_{1-1}q_1 - \frac{\rho^d_2}{\epsilon_2}F^s_{1-2}q_2.$$

While we could apply $i = 2$ to equation (6.20) to obtain a second equation for q_1 and q_2, it is simpler here to use *overall conservation of energy*, or $q_2 = -q_1$. Thus,

$$q_1 = \frac{\left[1-(1-\rho^s_1)F^s_{1-1}\right]E_{b1} - (1-\rho^s_2)F^s_{1-2}E_{b2}}{\dfrac{1}{\epsilon_1} - \dfrac{1-\epsilon_1-\rho^s_1}{\epsilon_1}F^s_{1-1} + \dfrac{1-\epsilon_2-\rho^s_2}{\epsilon_2}F^s_{1-2}}.$$

[2]Again, for easy readability of matrix manipulations we shall follow here the convention that a two-dimensional matrix is denoted by a bold capitalized letter, while a vector is written as a bold lowercase letter.

Using the results from Example 6.1 and dividing both numerator and denominator by F^s_{1-2}, we obtain

$$q_1 = \frac{(1-\rho_2^s)F^s_{1-2}(E_{b1}-E_{b2})}{\left(\frac{1}{\epsilon_1}+\frac{1}{\epsilon_2}\right)(1-\rho_2^s)F^s_{1-2}+F^s_{1-1}-F^s_{1-2}} = \frac{(1-\rho_2^s)(1)(E_{b1}-E_{b2})}{\left(\frac{1}{\epsilon_1}+\frac{1}{\epsilon_2}\right)(1-\rho_2^s)(1)+\rho_2^s-1} = \frac{E_{b1}-E_{b2}}{\frac{1}{\epsilon_1}+\frac{1}{\epsilon_2}-1}, \tag{6.25}$$

which produces the same result whether we have diffusely or specularly reflecting surfaces. Indeed, equation (6.25) is valid for the radiative transfer between two isothermal parallel plates, regardless of the directional behavior of the reflectance (i.e., it is not limited to the idealized reflectances considered in this chapter). *Any* beam leaving A_1 *must* hit surface A_2 and vice versa, regardless of whether the reflectance is diffuse, specular, or neither of the two; the surface locations will be different but the directional variation of reflectance has no influence on the heat transfer rate since the surfaces are isothermal.

Example 6.4. Repeat the previous example for concentric spheres and cylinders.

Solution
Again, from equation (6.20) with $i = 1$ and $H^s_{oi} = 0$, we obtain

$$E_{b1}-(1-\rho_1^s)F^s_{1-1}E_{b1}-(1-\rho_2^s)F^s_{1-2}E_{b2} = \frac{q_1}{\epsilon_1}-\frac{\rho_1^d}{\epsilon_1}F^s_{1-1}q_1-\frac{\rho_2^d}{\epsilon_2}F^s_{1-2}q_2.$$

In this case conservation of energy demands $q_2A_2 = -q_1A_1$, and

$$q_1 = \frac{\left[1-(1-\rho_1^s)F^s_{1-1}\right]E_{b1}-(1-\rho_2^s)F^s_{1-2}E_{b2}}{\frac{1}{\epsilon_1}-\frac{1-\epsilon_1-\rho_1^s}{\epsilon_1}F^s_{1-1}+\frac{1-\epsilon_2-\rho_2^s}{\epsilon_2}\frac{A_1}{A_2}F^s_{1-2}} = \frac{(1-\rho_2^s)F^s_{1-2}(E_{b1}-E_{b2})}{\left(\frac{1}{\epsilon_1}+\frac{1}{\epsilon_2}\frac{A_1}{A_2}\right)(1-\rho_2^s)F^s_{1-2}+F^s_{1-1}-\frac{A_1}{A_2}F^s_{1-2}}.$$

The specular view factors F^s_{1-1} and F^s_{1-2} are the same as in the previous example (cf. Example 6.2), leading to

$$q_1 = \frac{E_{b1}-E_{b2}}{\frac{1}{\epsilon_1}+\frac{1}{\epsilon_2}\frac{A_1}{A_2}-\frac{A_1/A_2-\rho_2^s}{1-\rho_2^s}}. \tag{6.26}$$

We note that equation (6.26) does not depend on ρ_1^s: Again, any radiation reflected off surface A_1 *must* return to surface A_2, regardless of the directional behavior of its reflectance. If surface A_2 is purely specular ($\rho_2^s = 1-\epsilon_2$), all radiation from A_1 bounces back and forth between A_1 and A_2, and equation (6.26) reduces to equation (6.25), i.e., the heat flux between these concentric spheres or cylinders is the same as between parallel plates. On the other hand, if A_2 is diffuse ($\rho_2^s = 0$) equation (6.26) reduces to the purely diffuse case since the directional behavior of ρ_1 is irrelevant.

Example 6.5. A very long solar collector plate is to collect energy at a temperature of $T_1 = 350\,\mathrm{K}$. To improve its performance for off-normal solar incidence, a highly reflective surface is placed next to the collector as shown in Fig. 6-7. For simplicity you may make the following assumptions: The collector is isothermal and gray-diffuse with emittance $\epsilon_1 = 1-\rho_1^d = 0.8$; the mirror is gray and specular with $\epsilon_2 = 1-\rho_2^s = 0.1$, and heat losses from the mirror by convection as well as all losses from the collector ends may be neglected. How much energy (per unit length) does the collector plate collect for solar irradiation of $q_{\mathrm{sun}} = 1000\,\mathrm{W/m^2}$ at an incidence angle of 30°?

Solution
Applying equation (6.22) to the absorber plate ($i = 1$) as well as the mirror ($i = 2$) we obtain

$$\left[1-(1-\rho_1^s)F^s_{1-1}\right]E_{b1}-(1-\rho_2^s)F^s_{1-2}E_{b2} = \left[\frac{1}{\epsilon_1}-\frac{\rho_1^d}{\epsilon_1}F^s_{1-1}\right]q_1-\frac{\rho_2^d}{\epsilon_2}F^s_{1-2}q_2+H^s_{o1},$$

$$-(1-\rho_1^s)F^s_{2-1}E_{b1}+\left[1-(1-\rho_2^s)F^s_{2-2}\right]E_{b2} = -\frac{\rho_1^d}{\epsilon_1}F^s_{2-1}q_1+\left[\frac{1}{\epsilon_2}-\frac{\rho_2^d}{\epsilon_2}F^s_{2-2}\right]q_2+H^s_{o2}.$$

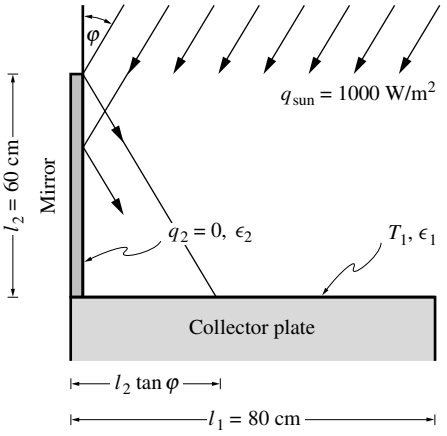

FIGURE 6-7
Geometry for Example 6.5.

Since $\rho_1^s = 0$, it follows that $F_{1-1}^s = F_{2-2}^s = 0$ and also $F_{1-2}^s = F_{1-2}$, $F_{2-1}^s = F_{2-1}$. For this configuration no specular reflections from one surface to another surface are possible (radiation leaving the absorber plate, after specular reflection from the mirror, always leaves the open enclosure). Thus, with $q_2 = 0$,

$$\begin{aligned} E_{b1} - \epsilon_2 F_{1-2} E_{b2} &= \frac{q_1}{\epsilon_1} + H_{o1}^s, \\ -F_{2-1} E_{b1} + E_{b2} &= -\left(\frac{1}{\epsilon_1} - 1\right) F_{2-1} q_1 + H_{o2}^s. \end{aligned}$$

Eliminating E_{b2}, by multiplying the second equation by $\epsilon_2 F_{1-2}$ and adding, leads to

$$(1 - \epsilon_2 F_{1-2} F_{2-1}) E_{b1} = \left[\frac{1}{\epsilon_1} - \left(\frac{1}{\epsilon_1} - 1\right) \epsilon_2 F_{1-2} F_{2-1}\right] q_1 + H_{o1}^s + \epsilon_2 F_{1-2} H_{o2}^s.$$

The external fluxes are evaluated as follows: The mirror receives solar flux only directly (no specular reflection off the absorber plate is possible), i.e., $H_{o2}^s = q_{sun} \sin \varphi$. The absorber plate receives a direct contribution, $q_{sun} \cos \varphi$, and a second contribution after specular reflection off the mirror. This second contribution has the strength of $\rho_2^s q_{sun} \cos \varphi$ per unit area. However, only part of the collector plate ($l_2 \tan \varphi$) receives this secondary contribution, which, for our crude two-node description, must be averaged over l_1. Thus,

$$H_{o1}^s = q_{sun} \cos \varphi + \rho_2^s q_{sun} \cos \varphi \frac{l_2 \tan \varphi}{l_1} = q_{sun} \left[\cos \varphi + (1 - \epsilon_2) \frac{l_2}{l_1} \sin \varphi\right].$$

Therefore,

$$q_1 = \frac{(1 - \epsilon_2 F_{1-2} F_{2-1}) E_{b1} - [\cos \varphi + (1 - \epsilon_2) \sin \varphi (l_2/l_1) + \epsilon_2 F_{1-2} \sin \varphi] q_{sun}}{\dfrac{1}{\epsilon_1} - \epsilon_2 \left(\dfrac{1}{\epsilon_1} - 1\right) F_{1-2} F_{2-1}}.$$

The view factors are readily evaluated by the crossed-strings method as $F_{1-2} = (80 + 60 - 100)/(2 \times 80) = \frac{1}{4}$ and $F_{2-1} = 80 \times \frac{1}{4}/60 = \frac{1}{3}$. Substituting numbers, we obtain

$$q_1 = \frac{\left(1 - 0.1 \times \frac{1}{4} \times \frac{1}{3}\right) 5.670 \times 10^{-8} \times 350^4 - \left(\frac{\sqrt{3}}{2} + 0.9 \times \frac{1}{2} \times \frac{60}{80} + 0.1 \times \frac{1}{4} \times \frac{1}{2}\right) 1000}{\frac{1}{0.8} - 0.1 \left(\frac{1}{0.8} - 1\right) \times \frac{1}{4} \times \frac{1}{3}} = -298 \text{ W/m}^2.$$

Under these conditions, therefore, the collector is about 30% efficient. This result should be compared with a collector without a mirror ($l_2 = 0$ and $F_{1-2} = 0$), for which we get

$$q_{1,\text{no mirror}} = \frac{E_{b1} - q_{sun} \cos \varphi}{1/\epsilon_1} = 0.8 \times \left(5.670 \times 10^{-8} \times 350^4 - 1000 \times \frac{\sqrt{3}}{2}\right) = -12 \text{ W/m}^2.$$

This absorber plate collects hardly any energy at all (indeed, after accounting for convection losses, it would experience a net energy loss). If the mirror had been a diffuse reflector the heat gain would have

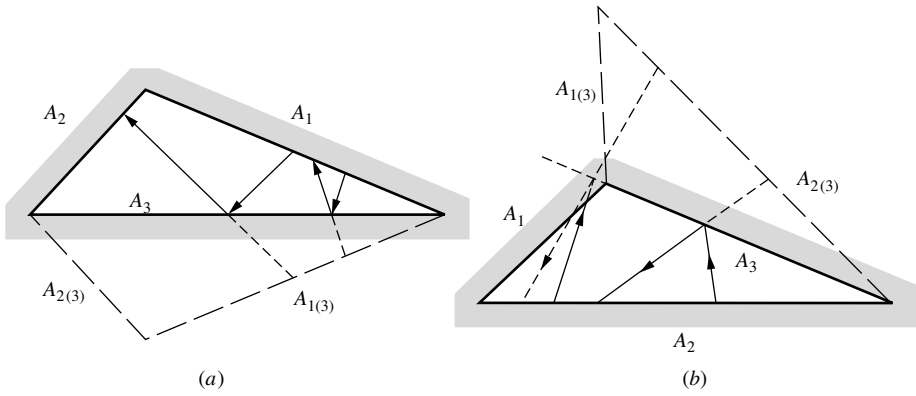

FIGURE 6-8
Triangular enclosure with a single specularly reflecting surface, with a few possible beam paths indicated, (*a*) without obstructions, (*b*) with partial obstructions.

been $q_{1,\text{diffuse mirror}} = -172\,\text{W/m}^2$, which is significantly less than for the specular mirror (cf. Problem 5.22).

We conclude from this example that (*i*) mirrors can significantly improve collector performance, and (*ii*) infrared reradiation losses from near-black collectors are very substantial. Of course, reradiation losses may be significantly reduced by using *selective surfaces* or glass-covered collectors (cf. Chapter 3).

We shall conclude this section with three more examples designed to clarify certain aspects of evaluating the specular view factors in enclosures comprised of only simple planar elements.

Example 6.6. Consider the triangular enclosures shown in Figs. 6-8*a* and *b*. Surfaces A_1 and A_2 are isothermal at T_1 and T_2, respectively, and are purely diffuse reflectors with $\epsilon_1 = 1 - \rho_1^d$ and $\epsilon_2 = 1 - \rho_2^d$. Surface A_3 is isothermal at T_3 and is a purely specular reflector with $\epsilon_3 = 1 - \rho_3^s$. Set up the system of equations for the unknown surface heat fluxes.

Solution
Since there is only a single (and flat) specular surface, no multiple specular reflections are possible. While F^s_{1-1} and F^s_{2-2} are nonzero, it is clear that $F^s_{3-3} = 0$. Thus, from equation (6.22), with $H^s_{oi} = 0$,

$$(1 - F^s_{1-1})E_{b1} - F^s_{1-2}E_{b2} - \epsilon_3 F^s_{1-3}E_{b3} = \left[\frac{1}{\epsilon_1} - \left(\frac{1}{\epsilon_1} - 1\right)F^s_{1-1}\right]q_1 - \left(\frac{1}{\epsilon_2} - 1\right)F^s_{1-2}q_2,$$

$$-F^s_{2-1}E_{b1} + (1 - F^s_{2-2})E_{b2} - \epsilon_3 F^s_{2-3}E_{b3} = -\left(\frac{1}{\epsilon_1} - 1\right)F^s_{2-1}q_1 + \left[\frac{1}{\epsilon_2} - \left(\frac{1}{\epsilon_2} - 1\right)F^s_{2-2}\right]q_2,$$

$$-F^s_{3-1}E_{b1} - F^s_{3-2}E_{b2} + E_{b3} = -\left(\frac{1}{\epsilon_1} - 1\right)F^s_{3-1}q_1 - \left(\frac{1}{\epsilon_2} - 1\right)F^s_{3-2}q_2 + \frac{q_3}{\epsilon_3}.$$

We note that q_3 only enters the last equation, so we only have two simultaneous equations to solve (i.e., as many as we have surfaces with *diffuse* reflection components). We shall need to determine the specular view factors F^s_{1-1}, F^s_{1-2}, and F^s_{2-2}, while the rest can be evaluated through reciprocity and the summation rule. Considering the first case of Fig. 6-8*a*, we find

$$\begin{aligned}
F^s_{1-1} &= \rho^s_3 F_{1(3)-1},\\
F^s_{1-2} &= F_{1-2} + \rho^s_3 F_{1(3)-2}, \quad \epsilon_3 F^s_{1-3} = 1 - F^s_{1-1} - F^s_{1-2},\\
F^s_{2-1} &= A_1 F^s_{1-2}/A_2,\\
F^s_{2-2} &= \rho^s_3 F_{2(3)-2}, \quad \epsilon_3 F^s_{2-3} = 1 - F^s_{2-1} - F^s_{2-2},\\
F^s_{3-1} &= A_1 F^s_{1-3}/A_3, \quad F^s_{3-2} = A_2 F^s_{2-3}/A_3,
\end{aligned}$$

where all view factors on the right-hand sides are readily evaluated through standard diffuse view factor analysis. The problem becomes slightly more difficult in the configuration shown in Fig. 6-8*b*, where the specular surface is attached to another surface with an opening angle of $> 90°$. Standing in the left corner on surface A_2, one obviously cannot see all of the image $A_{2(3)}$ from there by looking through

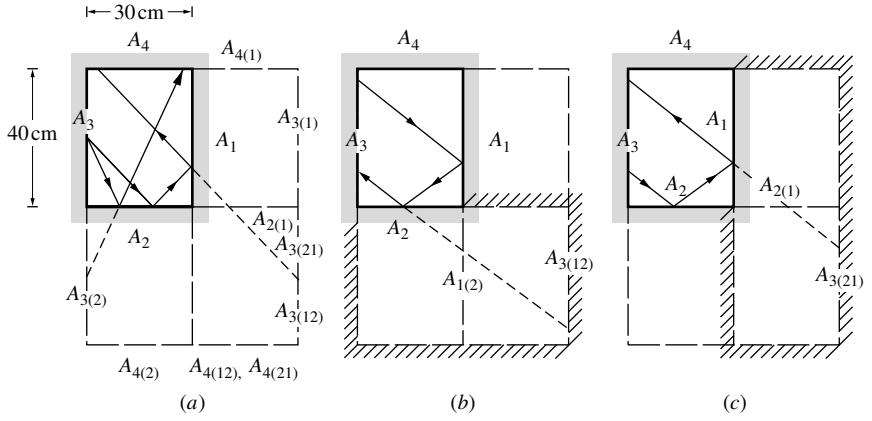

FIGURE 6-9
Rectangular enclosure with two adjacent specular reflectors, with some possible beam paths indicated: (*a*) evaluation of F^s_{3-4}, (*b*) evaluation of $A_{3(12)}$ contribution to F^s_{3-3}, (*c*) evaluation of $A_{3(21)}$ contribution to F^s_{3-3}.

"mirror" A_3. Care must be taken that these visual obstructions are not overlooked. If the enclosure is two-dimensional, such partially obstructed view factors are no problem for the crossed-strings method, but may pose great difficulty for an analytical solution otherwise.

The effects of partial shading become somewhat more obvious when configurations with two or more adjacent specular surfaces are considered.

Example 6.7. Consider the rectangular enclosure shown in Fig. 6-9. Surfaces A_1 and A_2 are purely specular, and surfaces A_3 and A_4 are purely diffuse reflectors. Top and bottom walls are at $T_1 = T_3 = 1000\,\text{K}$, with $\epsilon_1 = 1 - \rho^s_1 = \epsilon_3 = 1 - \rho^d_3 = 0.3$; the side walls are at $T_2 = T_4 = 600\,\text{K}$ with emittances $\epsilon_2 = 1 - \rho^s_2 = \epsilon_4 = 1 - \rho^d_4 = 0.8$. Determine the net radiative heat flux for each surface.

Solution
Looking at Fig. 6-9*a*, one sees that $F^s_{1-1} = F^s_{2-2} = 0$, while all other specular view factors are nonzero. Again, with $H^s_{oi} = 0$, we have from equation (6.22)

$$E_{b1} - \epsilon_2 F^s_{1-2} E_{b2} - F^s_{1-3} E_{b3} - F^s_{1-4} E_{b4} = \frac{q_1}{\epsilon_1} - \left(\frac{1}{\epsilon_3} - 1\right) F^s_{1-3} q_3 - \left(\frac{1}{\epsilon_4} - 1\right) F^s_{1-4} q_4,$$

$$-\epsilon_1 F^s_{2-1} E_{b1} + E_{b2} - F^s_{2-3} E_{b3} - F^s_{2-4} E_{b4} = \frac{q_2}{\epsilon_2} - \left(\frac{1}{\epsilon_3} - 1\right) F^s_{2-3} q_3 - \left(\frac{1}{\epsilon_4} - 1\right) F^s_{2-4} q_4,$$

$$-\epsilon_1 F^s_{3-1} E_{b1} - \epsilon_2 F^s_{3-2} E_{b2} + (1 - F^s_{3-3}) E_{b3} - F^s_{3-4} E_{b4} = \left[\frac{1}{\epsilon_3} - \left(\frac{1}{\epsilon_3} - 1\right) F^s_{3-3}\right] q_3 - \left(\frac{1}{\epsilon_4} - 1\right) F^s_{3-4} q_4,$$

$$-\epsilon_1 F^s_{4-1} E_{b1} - \epsilon_2 F^s_{4-2} E_{b2} - F^s_{4-3} E_{b3} + (1 - F^s_{4-4}) E_{b4} = -\left(\frac{1}{\epsilon_3} - 1\right) F^s_{4-3} q_3 + \left[\frac{1}{\epsilon_4} - \left(\frac{1}{\epsilon_4} - 1\right) F^s_{4-4}\right] q_4.$$

Again, we have only two simultaneous equations to solve for the two (diffuse) heat fluxes q_3 and q_4: The first two equations are explicit expressions for q_1 and q_2, respectively (once q_3 and q_4 have been determined). Checking the various images in Fig. 6-9*a*, we find that the specular view factors for surface A_1 are

$$\begin{aligned} F^s_{1-1} &= 0, \\ F^s_{1-2} &= F_{1-2}, \\ F^s_{1-3} &= F_{1-3} + \rho^s_2 F_{1(2)-3}, \\ F^s_{1-4} &= F_{1-4} + \rho^s_2 F_{1(2)-4}. \end{aligned}$$

Checking the summation rule, we find

$$(1 - \rho^s_1) F^s_{1-1} + (1 - \rho^s_2) F^s_{1-2} + F^s_{1-3} + F^s_{1-4} = 0 + F_{1-2} + F_{1-3} + F_{1-4} - \rho^s_2 (F_{1-2} - F_{1(2)-3} - F_{1(2)-4}) = 1$$

or

$$F_{1(2)-3} + F_{1(2)-4} = F_{1-2}.$$

Indeed, by checking Fig. 6-9*a*, we find

$$F_{1(2)-3} + F_{1(2)-4} = F_{1(2)-(3+4)} = F_{1(2)-2} = F_{1-2}.$$

Similarly, we have

$$\begin{aligned}
F^s_{2-2} &= 0,\\
F^s_{2-1} &= F_{2-1},\\
F^s_{2-3} &= F_{2-3} + \rho^s_1 F_{2(1)-3},\\
F^s_{2-4} &= F_{2-4} + \rho^s_1 F_{2(1)-4}.
\end{aligned}$$

For surfaces A_3 and A_4 dual specular reflections are possible:

$$\begin{aligned}
F^s_{3-1} &= F_{3-1} + \rho^s_2 F_{3(2)-1},\\
F^s_{3-2} &= F_{3-2} + \rho^s_1 F_{3(1)-2},\\
F^s_{3-3} &= \rho^s_1 F_{3(1)-3} + \rho^s_1\rho^s_2 F_{3(12)-3} + \rho^s_2\rho^s_1 F_{3(21)-3},\\
F^s_{3-4} &= F_{3-4} + \rho^s_1 F_{3(1)-4} + \rho^s_2 F_{3(2)-4} + \rho^s_1\rho^s_2 F_{3(12)-4} + \rho^s_2\rho^s_1 F_{3(21)-4},\\
F^s_{4-1} &= F_{4-1} + \rho^s_2 F_{4(2)-1},\\
F^s_{4-2} &= F_{4-2} + \rho^s_1 F_{4(1)-2},\\
F^s_{4-3} &= F_{4-3} + \rho^s_1 F_{4(1)-3} + \rho^s_2 F_{4(2)-3} + \rho^s_1\rho^s_2 F_{4(12)-3} + \rho^s_2\rho^s_1 F_{4(21)-3},\\
F^s_{4-4} &= \rho^s_2 F_{4(2)-4} + \rho^s_1\rho^s_2 F_{4(12)-4} + \rho^s_2\rho^s_1 F_{4(21)-4}.
\end{aligned}$$

It is tempting to assume that $F_{4(12)-4} = F_{4(21)-4}$, etc. Closer inspection of Figs. 6-9*b* and *c* reveals, however, that these view factors are partially obstructed: For example, for $F_{4(21)-4}$ all rays from $A_{4(21)}$ to A_4 must pass through the image $A_{2(1)}$ as well as A_1, i.e., all rays must stay *below* the corner between A_1 and A_2 (center point of Fig. 6-9*b*). On the other hand, for $F_{4(12)-4}$ all rays from $A_{4(12)}$ must stay *above* the corner between A_1 and A_2, and *both together* add up to the *unobstructed* view factor from the image to A_4. The same is true for $F_{3(12)-3} + F_{3(21)-3}$. However, the geometry is such that $F_{4(21)-3} = 0$, while $F_{4(12)-3}$ is unobstructed (thus, still adding up to the unobstructed view factor). Similarly, $F_{3(12)-4} = 0$, while $F_{3(21)-4}$ is unobstructed.

Simplifications for partially obstructed view factor were found for this particular simple geometry. Care must be taken before extrapolating these results to other configurations.

Before actually evaluating view factors one should take advantage of the fact that there are only two different surface temperatures, i.e., $E_{b3} = E_{b1}$ and $E_{b4} = E_{b2}$, and only two emittances, $\epsilon_3 = \epsilon_1$ and $\epsilon_4 = \epsilon_2$:

$$(1 - F^s_{1-3})E_{b1} - (\epsilon_2 F^s_{1-2} + F^s_{1-4})E_{b2} = \frac{q_1}{\epsilon_1} - \left(\frac{1}{\epsilon_1} - 1\right)F^s_{1-3}q_3 - \left(\frac{1}{\epsilon_2} - 1\right)F^s_{1-4}q_4,$$

$$-(\epsilon_1 F^s_{2-1} + F^s_{2-3})E_{b1} + (1 - F^s_{2-4})E_{b2} = \frac{q_2}{\epsilon_2} - \left(\frac{1}{\epsilon_1} - 1\right)F^s_{2-3}q_3 - \left(\frac{1}{\epsilon_2} - 1\right)F^s_{2-4}q_4,$$

$$(1 - \epsilon_1 F^s_{3-1} - F^s_{3-3})E_{b1} - (\epsilon_2 F^s_{3-2} + F^s_{3-4})E_{b2} = \left[\frac{1}{\epsilon_1} - \left(\frac{1}{\epsilon_1} - 1\right)F^s_{3-3}\right]q_3 - \left(\frac{1}{\epsilon_2} - 1\right)F^s_{3-4}q_4,$$

$$-(\epsilon_1 F^s_{4-1} + F^s_{4-3})E_{b1} + (1 - \epsilon_2 F^s_{4-2} - F^s_{4-4})E_{b2} = -\left(\frac{1}{\epsilon_1} - 1\right)F^s_{4-3}q_3 + \left[\frac{1}{\epsilon_2} - \left(\frac{1}{\epsilon_2} - 1\right)F^s_{4-4}\right]q_4.$$

The necessary view factors are readily found from the crossed-strings method [equation (4.50)], reciprocity, and the summation rule [equation (6.21)], as well as from Example 5.1 for the diffuse view factors:

$$\begin{aligned}
F^s_{1-2} &= F_{1-2} = 0.25;\\
&\qquad F_{1-3} = 0.5, \quad F_{1(2)-3} = (\sqrt{64+9} + 3 - 2\times 5)/2\times 4 = 0.1930:\\
F^s_{1-3} &= 0.5 + 0.2\times 0.1930 = 0.5386;\\
&\qquad F_{1-4} = 0.25, \quad F_{1(2)-4} = (5 + 8 - 4 - \sqrt{73})/8 = 0.0570:\\
F^s_{1-4} &= 0.25 + 0.2\times 0.0570 = 0.2614;\\
F^s_{2-1} &= F_{2-1} = 0.3333;
\end{aligned}$$

$$
\begin{aligned}
F_{2-3} &= 0.3333, \quad F_{2(1)-3} = (5+6-\sqrt{52}-3)/6 = 0.1315: \\
F^s_{2-3} &= 0.3333 + 0.7\times 0.1315 = 0.4254; \\
F_{2-4} &= 0.3333, \quad F_{2(1)-4} = (\sqrt{52}+4-2\times 5)/6 = 0.2019: \\
F^s_{2-4} &= 0.3333 + 0.7\times 0.2019 = 0.4746; \\
F^s_{3-1} &= F^s_{1-3} = 0.5386; \\
F^s_{3-2} &= A_2F^s_{2-3}/A_3 = 0.75\times 0.4254 = 0.3191; \\
F_{3(1)-3} &= (\sqrt{52}-6)/4 = 0.3028, \\
F_{3(12)-3} + F_{3(21)-3} &= (10+6-2\sqrt{52})/8 = 0.1972: \\
F^s_{3-3} &= 0.7\times 0.3028 + 0.2\times 0.7\times 0.1972 = 0.2396; \\
F^s_{3-4} &= 1-\epsilon_1F^s_{3-1}-\epsilon_2F^s_{3-2}-F^s_{3-3} \\
&= 1-0.3\times 0.5386-0.8\times 0.3191-0.2396 = 0.3436; \\
F^s_{4-1} &= A_1F^s_{1-4}/A_4 = 0.2614/0.75 = 0.3485; \\
F^s_{4-2} &= F^s_{2-4} = 0.4746; \\
F^s_{4-3} &= A_3F^s_{3-4}/A_4 = 0.3436/0.75 = 0.4581; \\
F^s_{4-4} &= 1-\epsilon_1F^s_{4-1}-\epsilon_2F^s_{4-2}-F^s_{4-3} \\
&= 1-0.3\times 0.3485-0.8\times 0.4746-0.4581 = 0.0576.
\end{aligned}
$$

Substituting these values into the heat flux equations and realizing, from the summation rule, that the two coefficients in front of E_{b1} and E_{b2} are the same for each equation, we obtain

$$
\begin{aligned}
(1-0.5386)(E_{b1}-E_{b2}) &= \frac{q_1}{0.3}-\left(\frac{1}{0.3}-1\right)0.5386q_3-\left(\frac{1}{0.8}-1\right)0.2614q_4, \\
-(1-0.4746)(E_{b1}-E_{b2}) &= \frac{q_2}{0.8}-\left(\frac{1}{0.3}-1\right)0.4254q_3-\left(\frac{1}{0.8}-1\right)0.4746q_4, \\
(0.8\times 0.3191+0.3436)(E_{b1}-E_{b2}) &= \left[\frac{1}{0.3}-\left(\frac{1}{0.3}-1\right)0.2396\right]q_3-\left(\frac{1}{0.8}-1\right)0.3436q_4, \\
-(0.3\times 0.3485+0.4581)(E_{b1}-E_{b2}) &= -\left(\frac{1}{0.3}-1\right)0.4581q_3+\left[\frac{1}{0.8}-\left(\frac{1}{0.8}-1\right)0.0576\right]q_4.
\end{aligned}
$$

After a little cleaning up these equations become

$$
\begin{aligned}
2.7743q_3-0.0859q_4 &= 0.5989(E_{b1}-E_{b2}), \\
-1.0689q_3+1.2356q_4 &= -0.5627(E_{b1}-E_{b2}), \\
q_1 &= 0.3770q_3+0.0196q_4+0.1384(E_{b1}-E_{b2}), \\
q_2 &= 0.7941q_3+0.0949q_4-0.4203(E_{b1}-E_{b2}).
\end{aligned}
$$

Solving the first two equations leads to

$$
\begin{aligned}
q_3 &= \frac{0.5989\times 1.2356-0.5627\times 0.0859}{2.7743\times 1.2356-1.0689\times 0.0859}(E_{b1}-E_{b2}) = 0.2073(E_{b1}-E_{b2}), \\
q_4 &= \frac{0.5989\times 1.0689-0.5627\times 2.7743}{2.7743\times 1.2356-1.0689\times 0.0859}(E_{b1}-E_{b2}) = -0.2761(E_{b1}-E_{b2}),
\end{aligned}
$$

and

$$
\begin{aligned}
q_1 &= [0.3770\times 0.2073+0.0196\times(-0.2761)+0.1384](E_{b1}-E_{b2}) = 0.2111(E_{b1}-E_{b2}), \\
q_2 &= [0.7941\times 0.2073+0.0949\times(-0.2761)-0.4203](E_{b1}-E_{b2}) = -0.2819(E_{b1}-E_{b2}).
\end{aligned}
$$

To determine the net surface heat fluxes we evaluate

$$
E_{b1}-E_{b2} = \sigma(T_1^4-T_2^4) = 5.670\times 10^{-8}(1000^4-600^4)\,\mathrm{W/m^2} = 4.935\,\mathrm{W/cm^2}
$$

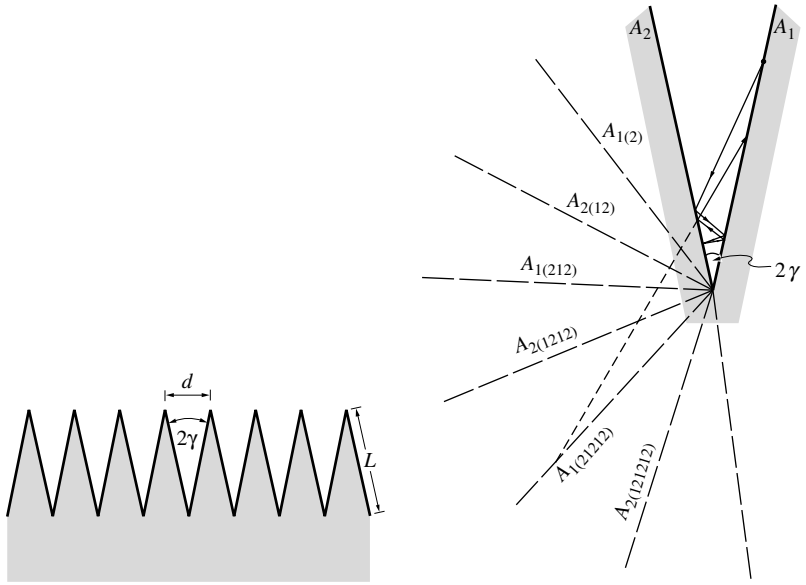

FIGURE 6-10
Geometry for Example 6.8: (*a*) V-corrugated surface, (*b*) images for a single V for the evaluation of F^s_{1-1}.

and multiply by the respective surface areas. Thus,

$$\begin{aligned} Q'_1 &= 40\,\text{cm} \times 0.2111 \times 4.935\,\text{W/cm}^2 = 41.7\,\text{W/cm}, \\ Q'_2 &= 30\,\text{cm} \times (-0.2819) \times 4.935\,\text{W/cm}^2 = -41.7\,\text{W/cm}, \\ Q'_3 &= 40\,\text{cm} \times 0.2073 \times 4.935\,\text{W/cm}^2 = 40.9\,\text{W/cm}, \\ Q'_4 &= 30\,\text{cm} \times (-0.2761) \times 4.935\,\text{W/cm}^2 = -40.9\,\text{W/cm}. \end{aligned}$$

Checking our results, we note that the four heat fluxes add up to zero as they should.

The results of the present example—an enclosure with two adjacent specular reflectors—should be compared with those of Example 5.4, dealing with the identical problem except that all four surfaces were perfectly diffuse reflectors. For Example 5.4, we had found $Q'_1 = -Q'_2 = Q'_3 = -Q'_4 = 42.3\,\text{W/cm}$. For the present configuration the heat fluxes of the specular surfaces are reduced by 1%, while the heat fluxes of the diffuse surfaces are reduced a little more, by approximately 3%. Overall, the effects of specularity are found to be rather minor.

In the last two examples only two simultaneous equations had to be solved, even though there were three and four unknown surface heat fluxes, respectively, because for any *purely specular surface with known temperature* the radiosity is not unknown, but is given as $J = \epsilon E_b$. Thus, for an enclosure consisting of N surfaces, of which n are purely specular with known temperature, only $N - n$ simultaneous equations need to be solved. While this fact simplifies specular enclosure analysis as compared with diffuse enclosures, one should remember that, in general, specular view factors are considerably more difficult to evaluate.

As a final example for configurations with flat surfaces we shall consider a case where many specular reflections are possible.

Example 6.8. Since solar energy strikes the absorbing plate of a strategically oriented solar collector only over a narrow band of incidence directions (varying somewhat during the day, as well as during the year), the ideal collector material would be directionally selective: The emittance should be high for directions of solar incidence (to maximize energy collection), and low for all other directions (to minimize reradiation losses). One such material is a V-corrugated specular surface shown in Fig. 6-10*a*. Assuming that the V-corrugated groove, with opening angle 2γ, is coated with a purely specular

reflecting material, with emittance $\epsilon = 1 - \rho^s$, what is the apparent hemispherical emittance of such a surface (i.e., what is its heat loss compared with a flat black plate at the same temperature)?

Solution

Calling the two surfaces in a single "V" A_1 and A_2, as indicated in Fig. 6-10*b*, with $E_{b1} = E_{b2} = E_b$, $\epsilon_1 = \epsilon_2 = \epsilon$, and $H^s_{o1} = H^s_{o2} = 0$ we obtain from equation (6.22) (for $i = 1$)

$$\left[1 - \epsilon\left(F^s_{1-1} + F^s_{1-2}\right)\right] E_b = \frac{q}{\epsilon}.$$

Total heat lost from both surfaces of the groove is $Q = q \times 2L = qd/\sin\gamma$; on the other hand, heat lost from a black surface covering the opening would be $Q_b = E_b d$. Thus, the apparent emittance is

$$\epsilon_a = \frac{Q}{Q_b} = \frac{q}{E_b \sin\gamma} = \frac{\epsilon\left[1 - \epsilon\left(F^s_{1-1} + F^s_{1-2}\right)\right]}{\sin\gamma}.$$

This expression could be further simplified, using summation rule and reciprocity, to $\epsilon_a = \epsilon F^s_{1-3}/\sin\gamma = 2\epsilon F^s_{3-1}$, where A_3 is the open top of the V (and of width d). However, F^s_{1-1} and F^s_{1-2} are somewhat simpler to evaluate, and we shall do so here: A beam leaving surface A_1 can return to A_1 (*i*) after a single reflection off surface A_2 [appearing to come from the image $A_{1(2)}$, as indicated in Fig. 6-10*b*], or (*ii*) after hitting A_2, traveling back to A_1, returning one more time to A_2, and hitting A_1 a second time [i.e., a beam that appears to come from image $A_{1(212)}$], and so on. Thus,

$$F^s_{1-1} = \rho F_{1(2)-1} + \rho^3 F_{1(212)-1} + \rho^5 F_{1(21212)-1} + \ldots.$$

F^s_{1-2} may be similarly evaluated. We shall here determine $F^s_{2-1} = F^s_{1-2}$ instead, since this expression allows us to employ the images shown in Fig. 6-10*b*: Energy may travel directly from A_2 to A_1, or go from A_2 to A_1, get reflected back to A_2, and reflected back to A_1 again [appearing to come from image $A_{2(12)}$], and so forth. Therefore,

$$F^s_{1-2} = F^s_{2-1} = F_{2-1} + \rho^2 F_{2(12)-1} + \rho^4 F_{2(1212)-1} + \ldots.$$

Adding both together and using reciprocity (with all areas being the same), we obtain

$$F^s_{1-1} + F^s_{1-2} = F_{1-2} + \rho F_{1-1(2)} + \rho^2 F_{1-2(12)} + \rho^3 F_{1-1(212)} + \ldots.$$

Each one of these view factors F_{i-j} is subject to the restriction that all beams from A_1 to the image A_j must pass through *all* the images between A_1 and A_j; however, in this geometry no partial obstruction occurs as seen from Fig. 6-10*b*. The series above ends as soon as the image can no longer be seen from A_1, i.e., when the opening angle between A_1 and the image exceeds 180°. The view factor for a V-groove with opening angle 2ϕ is, from Configuration 34 in Appendix D, $F_{2\phi} = 1 - \sin\phi$. Thus,

$$F^s_{1-1} + F^s_{1-2} = 1 - \sin\gamma + \rho(1 - \sin 2\gamma) + \rho^2(1 - \sin 3\gamma) + \ldots + \rho^{n-1}(1 - \sin n\gamma), \quad n\gamma < \pi/2.$$

Finally, the apparent hemispherical emittance of the V-corrugated surface is

$$\epsilon_a = \frac{\epsilon}{\sin\gamma}\left[1 - \epsilon\sum_{k=1}^{n}\rho^{k-1}(1 - \sin k\gamma)\right], \quad n < \pi/2\gamma.$$

Figure 6-11 shows the apparent hemispherical emittance of V-corrugated surfaces as a function of opening angle for a number of flat-surface emittances. Also shown in the figure is the normal emittance (or absorptance), which may also be calculated from equation (6.22) (left as an exercise). For example, for $\epsilon = 0.5$ and a groove opening angle of $\gamma = 30°$, the apparent hemispherical emittance (important for reradiation losses) is 0.72, and the normal emittance (important for solar energy collection) is 0.88. While the difference between these two values is not huge, the corrugated groove (*i*) helps to make the absorber plate more black, and (*ii*) substantially reduces the reradiation losses (by $\simeq 20\%$ for the $\epsilon = 0.5$, $\gamma = 30°$ surface). More detail about the radiative properties of V-corrugated grooves may be found in the papers by Eckert and Sparrow [4], Sparrow and Lin [5], and Hollands [6], and the book by Sparrow and Cess [7].

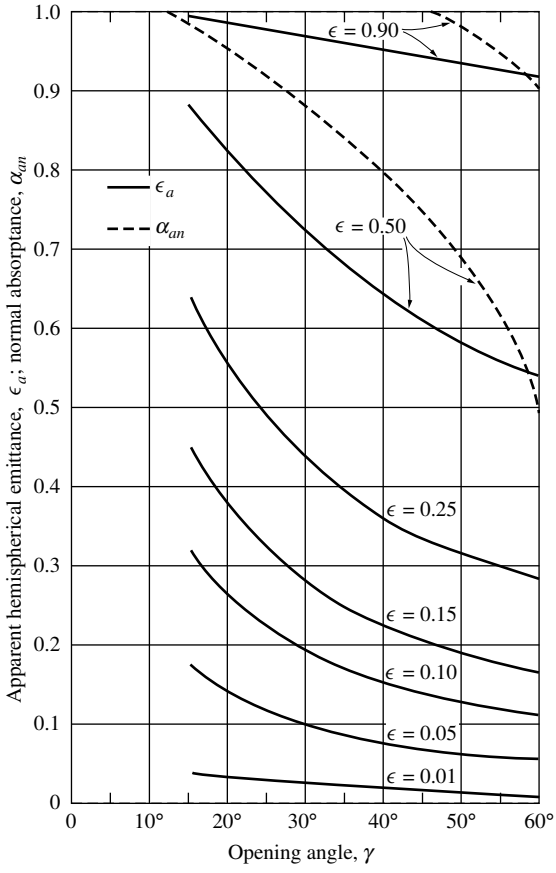

FIGURE 6-11
Apparent normal and hemispherical emittances for specularly reflecting V-corrugated surfaces [6].

Curved Surfaces with Specular Reflection Components

In all our examples we have only considered *idealized enclosures* consisting of *flat surfaces*, for which the mirror images necessary for specular view factor calculations are relatively easily determined. If some or all of the reflecting surfaces are *curved* then equations (6.18) and (6.20) remain valid, but the specular view factors tend to be much more difficult to obtain. Analytical solutions can be found only for relatively simple geometries, such as axisymmetric surfaces, but even then they tend to get very involved. The very simple case of cylindrical cavities (with and without specularly reflecting end plate) has been studied by Sparrow and coworkers [8–10] and by Perlmutter and Siegel [11]. The more involved case of conical cavities has been treated by Sparrow and colleagues [9,10,12] as well as Polgar and Howell [13], while spherical cavities have been addressed by Tsai and coworkers [14,15] and Sparrow and Jonsson [16,17]. Somewhat more generalized discussions on the determination of specular view factors for curved surfaces have been given by Plamondon and Horton [18] and by Burkhard and coworkers [19]. In view of the complexity involved in these evaluations, specular view factors for curved surfaces are probably most conveniently calculated by a statistical method, such as the Monte Carlo method, which will be discussed in detail in Chapter 8. A considerably more detailed discussion of thermal radiation from and within grooves and cavities is given in the book by Sparrow and Cess [7].

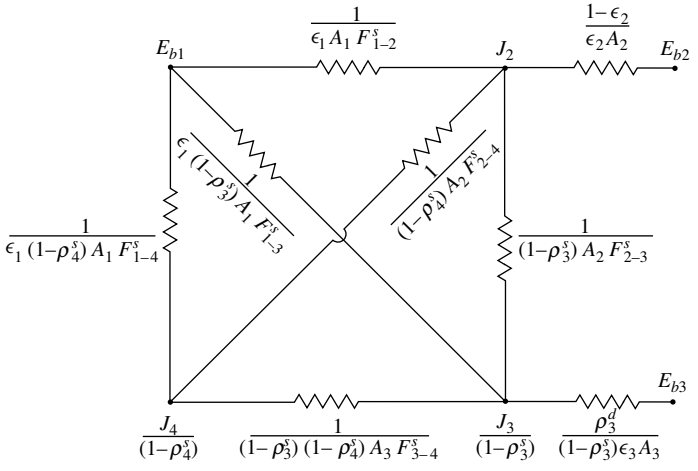

FIGURE 6-12
Electrical network equivalent for a four-surface enclosure (A_1 = specular, A_2 = diffuse, A_3 = partially diffuse and specular, A_4 = insulated, partially specular).

6.4 ELECTRICAL NETWORK ANALOGY

The electrical network analogy, first introduced in Section 5.4, may be readily extended to allow for partially specular reflectors. This possibility was first demonstrated by Ziering and Sarofim [20]. Expressing equations (6.12) and (6.15) for an idealized enclosure [i.e., an enclosure with finite surfaces of constant radiosity, exactly as was done in equation (6.19)], we can evaluate the nodal heat fluxes as

$$q_i = J_i - (1 - \rho_i^s)\left[\sum_{j=1}^{N} J_j F^s_{i-j} + H^s_{oi}\right], \quad i = 1, 2, \ldots, N. \tag{6.27}$$

Using the summation rule, equation (6.21), this relation may also be written as the sum of net radiative interchange between any two surfaces,

$$\begin{aligned} q_i &= \sum_{j=1}^{N} \left[(1 - \rho_j^s)J_i - (1 - \rho_i^s)J_j\right] F^s_{i-j} - (1 - \rho_i^s)H^s_{oi} \\ &= \sum_{j=1}^{N} \left[\frac{J_i}{1 - \rho_i^s} - \frac{J_j}{1 - \rho_j^s}\right](1 - \rho_i^s)(1 - \rho_j^s)F^s_{i-j} - (1 - \rho_i^s)H^s_{oi}. \end{aligned} \tag{6.28}$$

Similarly, from equation (6.13),

$$q_i = \frac{(1 - \rho_i^s)\epsilon_i}{\rho_i^d}\left(E_{bi} - \frac{J_i}{1 - \rho_i^s}\right). \tag{6.29}$$

After multiplication with A_i these relations may be combined and written in terms of potentials [E_{bi} and $J_i/(1 - \rho_i^s)$] and resistances as

$$Q_i = \frac{E_{bi} - \dfrac{J_i}{1 - \rho_i^s}}{\dfrac{\rho_i^d}{(1 - \rho_i^s)\epsilon_i A_i}} = \sum_{j=1}^{N} \frac{\dfrac{J_i}{1 - \rho_i^s} - \dfrac{J_j}{1 - \rho_j^s}}{\dfrac{1}{(1 - \rho_i^s)(1 - \rho_j^s)A_i F^s_{i-j}}} - (1 - \rho_i^s)\, A_i\, H^s_{oi}. \tag{6.30}$$

Of course, this relation reduces to equation (5.46) for the case of purely diffuse surfaces ($\rho_i^s = 0, \quad i = 1, 2, \ldots, N$). As an example, Fig. 6-12 shows the equivalent electrical network for an

enclosure consisting of four surfaces: Surface A_1 is a specular reflector ($\rho_1^d = 0$), surface A_2 is a diffuse reflector ($\rho_2^s = 0$), surface A_3 has specular and diffuse reflectance components, and surface A_4 (also partially specular) is insulated. Note that, unlike diffuse reflectance, the specular reflectance is *not* irrelevant for insulated surfaces.

6.5 RADIATION SHIELDS

As noted in Section 5.5 radiation shields tend to be made of specularly reflecting materials, such as polished metals or dielectric sheets coated with a metallic film. We would like, therefore, to extend the analysis to partly specular surfaces, i.e., (referring to Fig. 5-13) $\epsilon_k = 1 - \rho_k^s - \rho_k^d$ for all surfaces (inside and outside wall, all shield surfaces). Again, the analysis is most easily carried out using the electrical network analogy, and the resistance between any two layers has already been evaluated in Example 6.4, equation (6.26), as

$$R_{j-k} = \frac{1}{\epsilon_j A_j} + \frac{1}{\epsilon_k A_k} - \frac{1}{1-\rho_k^s}\left(\frac{1}{A_k} - \frac{\rho_k^s}{A_j}\right). \tag{6.31}$$

The resistances given in equation (6.31) may be simplified somewhat if surface A_k is either a purely diffuse reflector ($\rho_k^s = 0$), or a purely specular reflector ($1 - \rho_k^s = \epsilon_k$):

$$A_k \quad \text{diffuse}: \qquad R_{j-k} = \frac{1}{\epsilon_j A_j} + \left(\frac{1}{\epsilon_k} - 1\right)\frac{1}{A_k}, \tag{6.32a}$$

$$A_k \quad \text{specular}: \qquad R_{j-k} = \left(\frac{1}{\epsilon_j} + \frac{1}{\epsilon_k} - 1\right)\frac{1}{A_j}. \tag{6.32b}$$

Following the procedure of Section 5.5, equation (5.48) still holds, i.e.,

$$Q = \frac{E_{bi} - E_{bo}}{R_{i-1i} + \sum_{n=1}^{N-1} R_{no-n+1,i} + R_{No-o}}. \tag{6.33}$$

Example 6.9. Repeat Example 5.9 for purely specularly reflecting shields. The wall material (steel) may be diffusely or specularly reflecting.

Solution

As before we note from equation (6.32) that the resistances are inversely proportional to shield area, and will again assume $A_1 \simeq A_2 \simeq \ldots \simeq A_N = A_s = \pi D_s L$, with $D_s = 11\,\text{cm}$. Evaluating the total resistance from equations (6.33) and (6.32), we find

$$A_i R_{\text{tot}} = \frac{1}{\epsilon_w} + \left(\frac{1}{\epsilon_s} - 1\right)\frac{A_i^*}{A_s} + \sum_{n=1}^{N-1}\left(\frac{2}{\epsilon_s} - 1\right)\frac{A_i}{A_s} + \frac{1}{\epsilon_s}\frac{A_i}{A_s} + \left(\frac{1}{\epsilon_w} - 1\right)\frac{A_i}{A_o^*},$$

where, if the steel is specular $A_i^* = A_i$, $A_o^* = A_s$, and if it is diffuse $A_i^* = A_s$, $A_o^* = A_o$. We shall investigate both possibilities to see whether specularity of the steel is an important factor in this arrangement. Again, we may solve for N as

$$N = \frac{A_i R_{\text{tot}} - \frac{1}{\epsilon_w} - \left(\frac{1}{\epsilon_w} - 1\right)\frac{A_i}{A_o^*} + \left(\frac{1}{\epsilon_s} - 1\right)\left(\frac{A_i^*}{A_s} - \frac{A_i}{A_s}\right)}{\left(\frac{2}{\epsilon_s} - 1\right)\frac{A_i}{A_s}}$$

$$= \frac{580.0 - \frac{1}{0.3} - \left(\frac{1}{0.3} - 1\right)\frac{10}{11} - \left(\frac{1}{0.05} - 1\right)\left(1 - \frac{10}{11}\right)}{\left(\frac{2}{0.05} - 1\right)\frac{10}{11}} = 16.16, \qquad \text{steel specular,}$$

$$= \frac{580.0 - \frac{1}{0.3} - \left(\frac{1}{0.3} - 1\right)\frac{10}{20} - \left(\frac{1}{0.05} - 1\right)\left(\frac{10}{11} - \frac{10}{11}\right)}{\left(\frac{2}{0.05} - 1\right)\frac{10}{11}} = 16.23, \qquad \text{steel diffuse.}$$

Therefore, the same minimum of 17 radiation shields would be required. We note that the specularity of the shields has no impact whatsoever (because we assumed them to be infinitely close together in this analysis), while specular inner and outer cylinder walls marginally improve performance. Without radiation shields we obtain

$$q_i = \frac{|E_{bi} - E_{bo}|}{\frac{1}{\epsilon_w} + \left(\frac{1}{\epsilon_w} - 1\right) \times \left[1 \text{ or } \frac{A_i}{A_o}\right]} = \frac{5.670 \times 10^{-12} |4.2^4 - 298^4|}{\frac{1}{0.3} + \left(\frac{1}{0.3} - 1\right) \times [1 \text{ or } \frac{1}{2}]}$$

$$= \begin{cases} 9.94 \times 10^{-3}\ \mathrm{W/cm^2}, & \text{steel diffuse,} \\ 7.89 \times 10^{-3}\ \mathrm{W/cm^2}, & \text{steel specular,} \end{cases}$$

i.e, without shields the aspect ratio $A_i/A_o = 1/2$ deviates considerably from unity, making the differences between specular and diffuse cylinders more apparent.

6.6 SEMITRANSPARENT SHEETS (WINDOWS)

When we developed the governing relations for radiative heat transfer in an enclosure bounded by diffusely reflecting surfaces (Chapter 5) or by partially diffuse/partially specular reflectors (this chapter), we made allowance for external radiation to penetrate into the enclosure through holes and/or semitransparent surfaces (windows). While we have investigated some examples with external radiation entering through holes, only one (Example 5.8) has dealt with a simple semitransparent surface.

Radiative heat transfer in enclosures with semitransparent windows occurs in a number of important applications, such as solar collectors, externally irradiated specimens kept in a controlled atmosphere, furnaces with sight windows, and so on. We shall briefly outline in this section how such enclosures may be analyzed with equation (6.18) or (6.22). To this purpose we shall assume that properties of the semitransparent window are wavelength-independent (gray), that equation (6.1) describes the reflectance (facing the inside of the enclosure), and that the transmittance of the window also has specular (light is transmitted without change of direction) and diffuse (light leaving the window is perfectly diffuse) components.[3] Thus,

$$\rho + \tau + \alpha = \rho^s + \rho^d + \tau^s + \tau^d + \alpha = 1, \quad \epsilon = \alpha. \tag{6.34}$$

Further, we shall assume that radiation hitting the outside of the window has a collimated component q_{oc} (i.e., parallel rays coming from a single direction, such as sunshine) and a diffuse component q_{od} (such as sky radiation coming in from all directions with equal intensity). Making an energy balance for the *net radiative heat flux* from the semitransparent window into the enclosure leads to (cf. Fig. 6-13):

$$\begin{aligned} q(\mathbf{r}) &= q_{\text{em}} + q_{\text{tr,in}} - q_{\text{abs}} - q_{\text{tr,out}} \\ &= \epsilon(\mathbf{r}) E_b(\mathbf{r}) + \tau^d(\mathbf{r}) q_{oc}(\mathbf{r}) + \tau(\mathbf{r}) q_{od}(\mathbf{r}) - \alpha(\mathbf{r}) H(\mathbf{r}) - \tau(\mathbf{r}) H(\mathbf{r}), \end{aligned} \tag{6.35}$$

where the specularly transmitted fraction of the collimated external radiation, $\tau^s q_{oc}$, has not been accounted for since it enters the enclosure in a nondiffuse fashion; it is accounted for in $H_o^s(\mathbf{r}')$ as part of the irradiation at another enclosure location $\mathbf{r}'$ (traveling there directly, or after any number of specular reflections). Using equation (6.34), equation (6.35) may also be written as

$$q(\mathbf{r}) = q_{\text{out}} - q_{\text{in}} = \left(\epsilon E_b + \tau^d q_{oc} + \tau q_{od} + \rho^d H + \rho^s H\right) - H, \tag{6.36}$$

[3] It is unlikely that a realistic window has both specular and diffuse transmittance components; rather its transmittance will either be specular (clear windows) or diffuse (milky windows, glass blocks, etc.). We simply use the more general expression to make it valid for all types of windows.

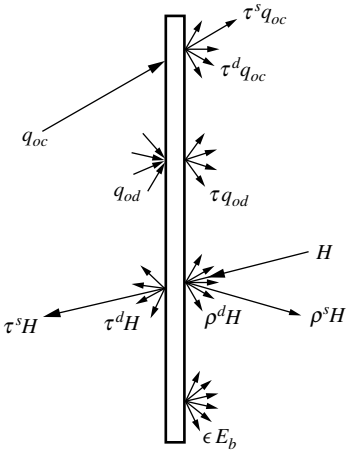

FIGURE 6-13
Energy balance for a semitransparent window.

where q_{in} is the energy falling onto the inside of the window coming from within the enclosure. The first four terms of q_{out} are diffuse and may be combined to form the radiosity

$$J(\mathbf{r}) = \epsilon E_b + \tau^d q_{oc} + \tau q_{od} + \rho^d H. \tag{6.37}$$

Examination of equations (6.34) through (6.37) shows that they may be reduced to equations (6.10) through (6.12) if we introduce an apparent emittance ϵ_a and an apparent blackbody emissive power $E_{b,a}$ as

$$\epsilon_a(\mathbf{r}) = \epsilon + \tau = 1 - \rho, \tag{6.38a}$$

$$\epsilon_a E_{b,a}(\mathbf{r}) = \epsilon E_b + \tau^d q_{oc} + \tau q_{od}. \tag{6.38b}$$

Thus, the semitransparent window is equivalent to an opaque surface with apparent emittance ϵ_a and apparent emissive power $E_{b,a}$ (if the radiative properties are *gray*). Therefore, equations (6.18) and (6.22) remain valid as long as the emittance and blackbody emissive powers of semitransparent surfaces are understood to be apparent values.

Example 6.10. A long hallway 3 m wide by 4 m high is lighted with a skylight that covers the entire ceiling. The skylight is double-glazed with an optical thickness of $\kappa d = 0.037$ per window plate. The floor and sides of the hallway may be assumed to be gray and diffuse with $\epsilon = 0.2$. The outside of the skylight is exposed to a clear sky, so that diffuse visible light in the amount of $q_{\text{sky}} = 20{,}000\,\text{lm/m}^2$ is incident on the skylight. Direct sunshine also falls on the skylight in the amount of $q_{\text{sun}} = 80{,}000\,\text{lm/m}^2$ (normal to the rays). For simplicity assume that the sun angle is $\theta_s = 36.87°$ as indicated in Fig. 6-14. Determine the amount of light incident on a point in the lower right-hand corner (also indicated in the figure) if (*a*) the skylight is clear, (*b*) the skylight is diffusing (with the same transmittance and reflectance).

Solution

From Fig. 3-32 for double glazing and $\kappa d = 0.037$ we find a hemispherical transmittance (i.e., directionally averaged) of $\tau \simeq 0.70$, while for solar incidence with $\theta = 36.87°$ we have $\tau_\theta \simeq 0.75$. The hemispherical reflectance of the skylight may be estimated by assuming that the reflectance is the same as the one of a nonabsorbing glass. Then, from Fig. 3-31 $\rho_1 = \rho_1^s = 1 - \tau(\kappa d = 0) \simeq 1 - 0.75 = 0.25$. From equation (6.38) we find $\epsilon_{1,a} = 1 - \rho_1 = 0.75$ and, for a clear skylight, $\epsilon_{1,a} E_{b1,a} = 0 + 0 + \tau q_{\text{sky}}$ since $\tau^d = 0$, and since there is no luminous emission from the window (or from any of the other walls, for that matter). Because of the special sun angle, direct sunshine falls only onto surface A_2, filling the entire wall, i.e., $H_{o2}^s = \tau_\theta q_{\text{sun}} \sin\theta_s$.

To determine the illumination at the point in the corner, we need to calculate the local irradiation H (in terms of *lumens*). This calculation, in turn, requires knowledge of the radiosity for all the surfaces of the hallway (for the skylight it is already known as $J_1 = \epsilon_{1,a} E_{b1,a} = \tau q_{\text{sky}}$, since $\rho_1^d = 0$). To this purpose we shall approximate the hallway as a four-surface enclosure for which we shall calculate the

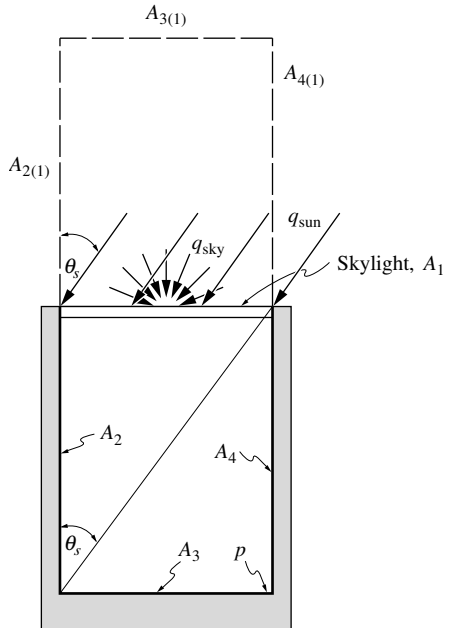

FIGURE 6-14
Geometry for a skylit hallway (Example 6.10).

average radiosities. Based on these radiosities we may then calculate the local irradiation for a point from equation (6.15). While equation (6.22) is most suitable for heat transfer calculations, we shall use equation (6.19) for this example since radiosities are more useful in lighting calculations.[4] Therefore, for $i = 2, 3$, and 4,

$$J_2 = \rho_2 \left(J_1 F^s_{2-1} + J_2 F^s_{2-2} + J_3 F^s_{2-3} + J_4 F^s_{2-4} \right) + H^s_{o2},$$
$$J_3 = \rho_3 \left(J_1 F^s_{3-1} + J_2 F^s_{3-2} + J_3 F^s_{3-3} + J_4 F^s_{3-4} \right),$$
$$J_4 = \rho_4 \left(J_1 F^s_{4-1} + J_2 F^s_{4-2} + J_3 F^s_{4-3} + J_4 F^s_{4-4} \right).$$

The necessary view factors are readily calculated from the crossed-strings method:

$$F^s_{2-1} = F_{2-1} = \frac{3 + 4 - 5}{2 \times 4} = 0.25, \qquad F^s_{2-2} = 0,$$

$$F^s_{2-3} = F_{2-3} + \rho_1 F_{2(1)-3} = 0.25 + 0.25 \times \frac{8+5-(4+\sqrt{73})}{2 \times 4} = 0.25(1+0.05700) = 0.26425,$$

$$F^s_{2-4} = F_{2-4} + \rho_1 F_{2(1)-4} = 0.5 + 0.25 \times \frac{3+\sqrt{73}-2 \times 5}{2 \times 4} = 0.5 + 0.25 \times 0.19300 = 0.54825,$$

$$F^s_{3-1} = F_{3-1} = \frac{2 \times 5 - 2 \times 4}{2 \times 3} = 0.33333,$$

$$F^s_{3-2} = \frac{A_2}{A_3} F^s_{2-3} = \frac{4}{3} \times 0.26425 = 0.35233,$$

$$F^s_{3-3} = \rho_1 F_{3(1)-3} = 0.25 \times \frac{2 \times \sqrt{73} - 2 \times 8}{2 \times 3} = 0.25 \times 0.18133 = 0.04533,$$

$$F^s_{3-4} = F^s_{3-2} = 0.35233,$$

$$F^s_{4-1} = F^s_{2-1} = 0.2500, \quad F^s_{4-2} = F^s_{2-4} = 0.54825,$$
$$F^s_{4-3} = F^s_{2-3} = 0.26425, \quad F^s_{4-4} = 0.$$

[4] If equation (6.22) is used the resulting heat fluxes are converted to radiosities using equation (6.13), or $J = -\rho^d q/\epsilon$ (since $E_b = 0$).

Therefore, after normalization with $\mathscr{J}_i = J_i/J_1$ and $\mathscr{H} = H^s_{o2}/J_1$, and with $\rho_2 = \rho_3 = \rho_4 = 1 - 0.2 = 0.8$,

$$\begin{aligned}
\mathscr{J}_2 &= 0.8(0.25 + 0 + 0.26425\ \mathscr{J}_3 + 0.54825\ \mathscr{J}_4) + \mathscr{H},\\
\mathscr{J}_3 &= 0.8(0.33333 + 0.35233\ \mathscr{J}_2 + 0.04533\ \mathscr{J}_3 + 0.35233\ \mathscr{J}_4),\\
\mathscr{J}_4 &= 0.8(0.25 + 0.54825\ \mathscr{J}_2 + 0.26425\ \mathscr{J}_3 + 0),
\end{aligned}$$

or

$$\begin{aligned}
\mathscr{J}_2 - 0.21140\ \mathscr{J}_3 - 0.43860\ \mathscr{J}_4 &= \mathscr{H} + 0.2,\\
-0.28186\ \mathscr{J}_2 + 0.96374\ \mathscr{J}_3 - 0.28186\ \mathscr{J}_4 &= 0.26667,\\
-0.43860\ \mathscr{J}_2 - 0.21140\ \mathscr{J}_3 + \mathscr{J}_4 &= 0.2.
\end{aligned}$$

Omitting the details of solving these three simultaneous equations, we find

$$\begin{aligned}
\mathscr{J}_2 &= 1.48978\mathscr{H} + 0.59051,\\
\mathscr{J}_3 &= 0.66812\mathscr{H} + 0.62211,\\
\mathscr{J}_4 &= 0.79466\mathscr{H} + 0.59051.
\end{aligned}$$

The irradiation onto the corner point is, from equation (6.15)

$$H_p = \sum_{j=1}^{4} J_j F^s_{p-j} = J_1\left(F^s_{p-1} + \mathscr{J}_2 F^s_{p-2} + \mathscr{J}_3 F^s_{p-3} + \mathscr{J}_4 F^s_{p-4}\right),$$

where the view factors may be determined from Configurations 10 and 11 in Appendix D (with $b \to \infty$, and multiplying by 2 since the strip tends to infinity in both directions):

$$\begin{aligned}
F^s_{p-1} &= F_{p-1} = \frac{1}{2}\frac{a}{\sqrt{a^2 + c^2}} = \frac{1}{2} \times \frac{3}{5} = 0.3,\\
F^s_{p-2} &= F_{p-2} + \rho_1 F_{p(1)-2} = F_{p-2} + \rho_1\left[F_{p(1)-2+2(1)} - F_{p(1)-2(1)}\right],\\
F_{p-2} &= \frac{1}{2}\left(1 - \frac{c}{\sqrt{a^2 + c^2}}\right) = \frac{1}{2}\left(1 - \frac{3}{5}\right) = 0.2,\\
F_{p(1)-2(1)} &= F_{p-2} = 0.2, \quad F_{p(1)-2+2(1)} = \frac{1}{2}\left(1 - \frac{3}{\sqrt{73}}\right) = 0.32444,\\
F^s_{p-2} &= 0.2 + 0.25 \times (0.32444 - 0.2) = 0.23111,\\
F^s_{p-3} &= \rho_1 F_{p(1)-3} = 0.25 \times \frac{1}{2} \times \frac{3}{\sqrt{73}} = 0.04389, \quad F^s_{p-4} = 0.5.
\end{aligned}$$

Therefore,

$$\begin{aligned}
\mathscr{H}_p = \frac{H_p}{J_1} &= 0.3 + 0.23111 \times (1.48978\mathscr{H} + 0.59051)\\
&\quad + 0.04389 \times (0.66812\mathscr{H} + 0.62211) + 0.5 \times (0.79466\mathscr{H} + 0.59051)\\
&= 0.77096\mathscr{H} + 0.75903.
\end{aligned}$$

Finally, for a clear window, $J_1 = \tau_1 q_{\text{sky}} = 0.7 \times 20{,}000 = 14{,}000\,\text{lx}$, and $H^s_{o2} = \tau_\theta q_{\text{sun}} \sin 36.87^\circ = 0.75 \times 80{,}000 \times 0.6 = 36{,}000\,\text{lx}$, and

$$H_p = 0.77096 \times 36{,}000 + 0.75903 \times 14{,}000 = 38{,}381\,\text{lx}.$$

On the other hand, if the window has a diffusing transmittance $\tau = \tau^d = 0.7$, then $H^s_{o2} = 0$ and, from equation (6.37), $J_1 = \tau(q_{\text{sky}} + q_{\text{sun}} \cos 36.87^\circ) = 0.7 \times (20{,}000 + 80{,}000 \times 0.8) = 58{,}800\,\text{lx}$. This results in

$$H_p = 0.75903 \times 58{,}800 = 44{,}631\,\text{lx}.$$

For a diffusing window the light is more evenly distributed throughout the hallway, resulting in higher illumination at point p.

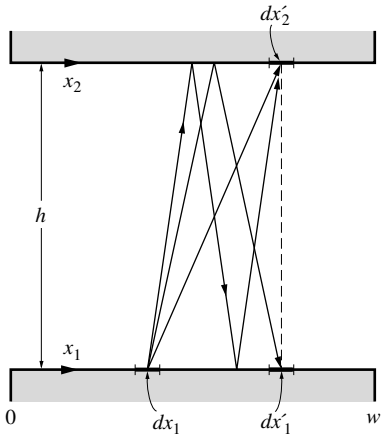

FIGURE 6-15
Radiative exchange between two long isothermal plates with specular reflection components.

6.7 SOLUTION OF THE GOVERNING INTEGRAL EQUATION

As in the case for diffusely reflecting surfaces the methods of the previous sections require the radiosity to be constant over each subsurface, a condition rarely met in practice. More accurate results may be obtained by solving the governing integral equation, either equation (6.16) (to determine radiosity J) or equation (6.18) (to determine the unknown heat flux and/or surface temperature directly), by any of the methods outlined in Chapter 5. This is best illustrated by repeating Examples 5.10 to 5.12.

Example 6.11. Consider two long parallel plates of width w as shown in Fig. 6-15. Both plates are isothermal at the (same) temperature T, and both have a gray, diffuse emittance of ϵ. The reflectance of the material is partly diffuse, partly specular, so that $\epsilon = 1 - \rho^s - \rho^d$. The plates are separated by a distance h and are placed in a large, cold environment. Determine the local radiative heat fluxes along the plate using numerical quadrature.

Solution
From equation (6.18) we find, for location x_1 on the lower plate,

$$E_b - (1-\rho^s)E_b\left[\int_0^w dF^s_{dx_1-dx_1'} + \int_0^w dF^s_{dx_1-dx_2'}\right] = \frac{q(x_1)}{\epsilon} - \frac{\rho^d}{\epsilon}\left[\int_0^w q(x_1')\,dF^s_{dx_1-dx_1'} + \int_0^w q(x_2')\,dF^s_{dx_1-dx_2'}\right].$$

The necessary specular view factors are readily found from

$$\begin{aligned} dF^s_{dx_1-dx_1'} &= \rho^s\,dF_{dx_1(2)-dx_1'} + (\rho^s)^3\,dF_{dx_1(212)-dx_1'} + \ldots, \\ dF^s_{dx_1-dx_2'} &= dF_{dx_1-dx_2'} + (\rho^s)^2\,dF_{dx_1(21)-dx_2'} + \ldots. \end{aligned}$$

The view factor between two infinitely long parallel strips of infinitesimal width and separated by a distance kh ($k = 1, 2, \ldots$) is given by Example 5.10 as

$$\frac{1}{2}\frac{(kh)^2\,dx'}{[(kh)^2 + (x-x')^2]^{3/2}}.$$

Thus,

$$\begin{aligned} dF^s_{dx_1-dx_1'} + dF^s_{dx_1-dx_2'} &= dF_{dx_1-dx_2'} + \rho^s\,dF_{dx_1(2)-dx_1'} + (\rho^s)^2\,dF_{dx_1(21)-dx_2'} + \ldots \\ &= \frac{1}{2}\sum_{k=1}^{\infty}(\rho^s)^{k-1}\frac{(kh)^2\,dx'}{[(kh)^2 + (x_1-x')^2]^{3/2}}, \end{aligned}$$

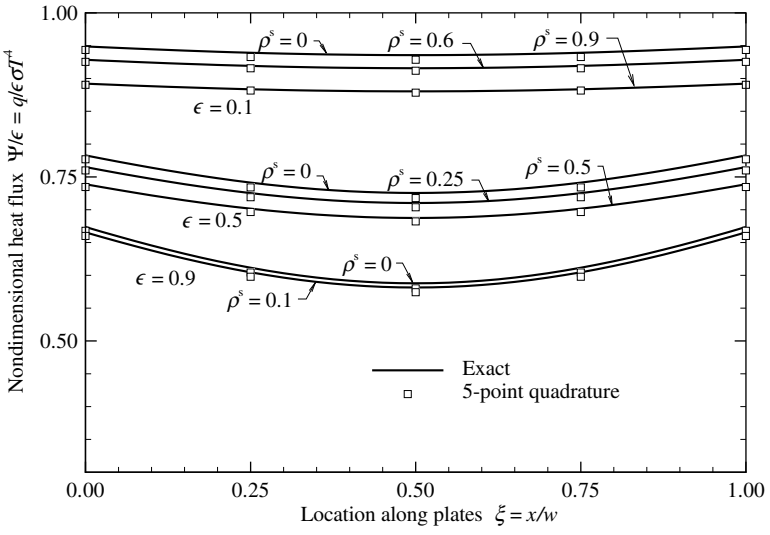

FIGURE 6-16
Local radiative heat flux on isothermal, parallel plates with diffuse and specular reflection components.

where we have made use of $x_1' = x_2' = x'$. This expression may be substituted into the governing integral equation. Realizing that, by symmetry, $q(x_1') = q(x_2') = q(x')$ and nondimensionalizing with $\xi = x/h$, $W = w/h$, and $\Psi = q(\xi)/E_b$, lead to

$$1 - (1-\rho^s)\int_0^W \frac{1}{2}\sum_{k=1}^{\infty} \frac{(\rho^s)^{k-1}k^2\,d\xi'}{[k^2+(\xi-\xi')^2]^{3/2}} = \frac{\Psi(\xi)}{\epsilon} - \frac{\rho^d}{\epsilon}\left[\int_0^W \Psi(\xi')\frac{1}{2}\sum_{k=1}^{\infty}\frac{(\rho^s)^{k-1}k^2\,d\xi'}{[k^2+(\xi-\xi')^2]^{3/2}}\right].$$

As in Example 5.11 this equation may be solved by numerical quadrature as

$$\Psi_i - \rho^d W\sum_{j=1}^{J} c_j\Psi_j f_{ij} = \epsilon\left[1-(1-\rho^s)W\sum_{j=1}^{J}c_j f_{ij}\right],$$

where Ψ_i is evaluated at J nodal positions ξ_i, $i = 1, 2, \ldots, J$, and the c_j are weight coefficients for the numerical integration. The f_{ij} are an abbreviation for the integration kernel,

$$f_{ij} = \frac{1}{2}\sum_{k=1}^{\infty}\frac{k^2(\rho^s)^{k-1}}{\left[k^2+(\xi_i-\xi_j)^2\right]^{3/2}}.$$

They must be evaluated by summing as many terms as necessary (decreasing as $(\rho^s)^{k-1}/k$ for large k). Results for the same simple $J = 5$ quadrature of Example 5.11 are given in Fig. 6-16, together with "exact" solutions (high-order quadrature). The results show that, for $W = w/h = 1$, the heat loss from the plates decreases if reflection is specular: Specular reflection traps emitted radiation somewhat more through repeated reflections between the plates.

Note that, if both surfaces are purely specular, the heat flux may be calculated directly (i.e., no solution of an integral equation is necessary). This calculation was first done for the parallel-plate case by Eckert and Sparrow [4]. In general, equation (6.18) is actually easier to solve than its diffuse-reflection counterpart if some or all of the surfaces are purely specular. However, the necessary specular view factors are generally much more difficult—if not impossible—to evaluate. Such a case arises, for example, for curved surfaces with multiple specular reflections. Since the specular view factors for such problems are most easily found from statistical methods, such as the Monte Carlo method (Chapter 8), it is usually best to solve the entire heat transfer problem using the Monte Carlo method.

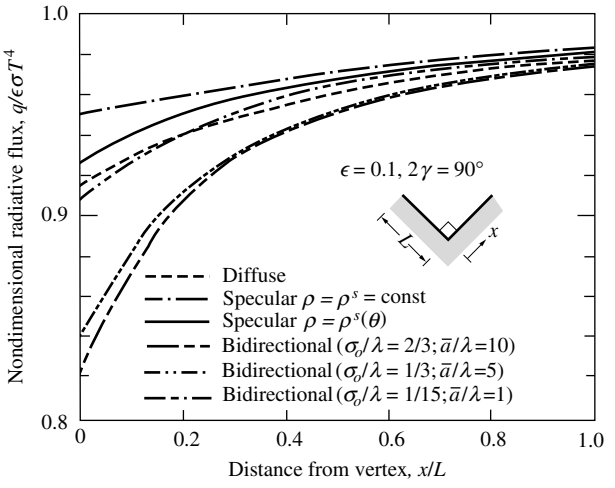

FIGURE 6-17
Local radiative heat flux from the surface of an isothermal V-groove for different reflection behavior; for all surfaces $2\gamma = 90°$ and $\epsilon = 0.1$; σ_o is root-mean-square optical roughness, $\bar{a}$ is a measure [21] for average distance between roughness peaks [22].

6.8 CONCLUDING REMARKS

Before leaving the topic of specularly reflecting surfaces we want to discuss briefly under what circumstances the assumption of a partly diffuse, partly specular reflector is appropriate. The analysis for such surfaces is generally considerably more involved than for diffusely reflecting surfaces, as a result of the more difficult evaluation of specular view factors. On the other hand, the analysis is substantially less involved than for surfaces with more irregular reflection behavior (as will be discussed in the following chapter).

Examples 6.3 and 6.7 have shown that in fully closed configurations (without external irradiation) the heat fluxes show very little dependence on specularity. This is true for all closed configurations as long as there are no long and narrow channels separating surfaces of widely different temperatures (cf. Problems 6.3 and 6.4). Therefore, for most practical enclosures it should be sufficient to evaluate heat fluxes assuming purely diffuse reflectors—even though a number of surfaces may be decidedly specular. On the other hand, in open configurations, in long and narrow channels, in configurations with collimated irradiation—whenever there is a possibility of *beam channeling*—the influence of specularity can be very substantial and must be accounted for.

It is tempting to think of diffuse and specular reflection as not only *extreme* but also *limiting* cases: This leads to the thought that—if heat fluxes have been determined for purely diffuse reflection, and again for purely specular reflection—the heat flux for a surface with more irregular reflection behavior must always lie between these two limiting values. This consideration is true in most cases, in particular since most real surfaces tend to have a reflectance maximum near the specular direction. However, there are cases when the actual heat flux is *not* bracketed by the diffuse and specular reflection models, particularly for directionally selective surfaces. As an example consider the local radiative heat flux from an isothermal groove, such as the one given by Fig. 6-10. Toor [22] has investigated this problem for diffuse reflectors, for specular reflectors, and for three different types of surface roughnesses analyzed with the Monte Carlo method, and his results are shown in Fig. 6-17. It is quite apparent that, near the vertex of the groove, diffuse and specular reflectors both seriously overpredict the heat loss. The reason is that, at grazing angles, rough surfaces tend to reflect strongly back into the direction of incidence.

References

1. Sarofim, A. F., and H. C. Hottel: "Radiation exchange among non-Lambert surfaces," *ASME Journal of Heat Transfer*, vol. 88, pp. 37–44, 1966.
2. Birkebak, R. C., E. M. Sparrow, E. R. G. Eckert, and J. W. Ramsey: "Effect of surface roughness on the total and specular reflectance of metallic surfaces," *ASME Journal of Heat Transfer*, vol. 86, pp. 193–199, 1964.

3. Wylie, C. R.: *Advanced Engineering Mathematics*, 5th ed., McGraw-Hill, New York, 1982.
4. Eckert, E. R. G., and E. M. Sparrow: "Radiative heat exchange between surfaces with specular reflection," *International Journal of Heat and Mass Transfer*, vol. 3, pp. 42–54, 1961.
5. Sparrow, E. M., and S. L. Lin: "Absorption of thermal radiation in v-groove cavities," *International Journal of Heat and Mass Transfer*, vol. 5, pp. 1111–1115, 1962.
6. Hollands, K. G. T.: "Directional selectivity, emittance, and absorptance properties of vee corrugated specular surfaces," *Solar Energy*, vol. 7, no. 3, pp. 108–116, 1963.
7. Sparrow, E. M., and R. D. Cess: *Radiation Heat Transfer*, Hemisphere, New York, 1978.
8. Sparrow, E. M., L. U. Albers, and E. R. G. Eckert: "Thermal radiation characteristics of cylindrical enclosures," *ASME Journal of Heat Transfer*, vol. 84, pp. 73–81, 1962.
9. Lin, S. H., and E. M. Sparrow: "Radiant interchange among curved specularly reflecting surfaces, application to cylindrical and conical cavities," *ASME Journal of Heat Transfer*, vol. 87, pp. 299–307, 1965.
10. Sparrow, E. M., and S. L. Lin: "Radiation heat transfer at a surface having both specular and diffuse reflectance components," *International Journal of Heat and Mass Transfer*, vol. 8, pp. 769–779, 1965.
11. Perlmutter, M., and R. Siegel: "Effect of specularly reflecting gray surface on thermal radiation through a tube and from its heated wall," *ASME Journal of Heat Transfer*, vol. 85, pp. 55–62, 1963.
12. Sparrow, E. M., and V. K. Jonsson: "Radiant emission characteristics of diffuse conical cavities," *Journal of the Optical Society of America*, vol. 53, pp. 816–821, 1963.
13. Polgar, L. G., and J. R. Howell: "Directional thermal-radiative properties of conical cavities," *NASA TN D-2904*, 1965.
14. Tsai, D. S., F. G. Ho, and W. Strieder: "Specular reflection in radiant heat transport across a spherical void," *Chemical Engineering Science–Genie Chimique*, vol. 39, pp. 775–779, 1984.
15. Tsai, D. S., and W. Strieder: "Radiation across a spherical cavity having both specular and diffuse reflectance components," *Chemical Engineering and Science*, vol. 40, no. 1, p. 170, 1985.
16. Sparrow, E. M., and V. K. Jonsson: "Absorption and emission characteristics of diffuse spherical enclosures," *NASA TN D-1289*, 1962.
17. Sparrow, E. M., and V. K. Jonsson: "Absorption and emission characteristics of diffuse spherical enclosures," *ASME Journal of Heat Transfer*, vol. 84, pp. 188–189, 1962.
18. Plamondon, J. A., and T. E. Horton: "On the determination of the view function to the images of a surface in a nonplanar specular reflector," *International Journal of Heat and Mass Transfer*, vol. 10, no. 5, pp. 665–679, 1967.
19. Burkhard, D. G., D. L. Shealy, and R. U. Sexl: "Specular reflection of heat radiation from an arbitrary reflector surface to an arbitrary receiver surface," *International Journal of Heat and Mass Transfer*, vol. 16, pp. 271–280, 1973.
20. Ziering, M. B., and A. F. Sarofim: "The electrical network analog to radiative transfer: Allowance for specular reflection," *ASME Journal of Heat Transfer*, vol. 88, pp. 341–342, 1966.
21. Beckmann, P., and A. Spizzichino: *The Scattering of Electromagnetic Waves from Rough Surfaces*, Macmillan, New York, 1963.
22. Toor, J. S.: "Radiant heat transfer analysis among surfaces having direction dependent properties by the Monte Carlo method," M.S. thesis, Purdue University, Lafayette, IN, 1967.

Problems

6.1 An infinitely long, diffusely reflecting cylinder is opposite a large, infinitely long plate of semiinfinite width (in plane of paper) as shown in the adjacent sketch. The plate is specularly reflecting with $\rho_2^s = 0.5$. As the center of the cylinder moves from $x = +\infty$ to $x = -\infty$ plot F_{1-1}^s vs. position h (your plot should include at least three precise values).

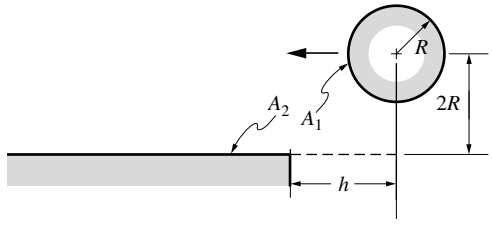

6.2 Consider two identical conical cavities (such as the ones depicted next to Problems 6.7 and 6.8), which are identical except for their surface treatment, making one surface a diffuse and the other a specular reflector. If both cones are isothermal, and both lose the same total amount of heat by radiation, which one has the higher temperature?

6.3 Two infinitely long black plates of width D are separated by a long, narrow channel, as indicated in the adjacent sketch. One plate is isothermal at T_1, the other is isothermal at T_2. The emittance of the insulated channel wall is ϵ. Determine the radiative heat flux between the plates if the channel wall is (*a*) specular, (*b*) diffuse. For simplicity you may treat the channel wall as a single node. The diffuse case approximates the behavior of a *light guide*, a device used to pipe daylight into interior, windowless spaces.

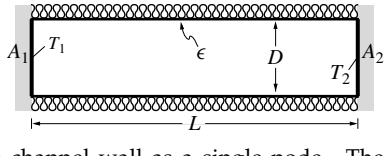

6.4 Two circular black plates of diameter D are separated by a long, narrow tubular channel, as indicated in the sketch next to Problem 6.3. One disk is isothermal at T_1, the other is isothermal at T_2. The channel wall is a perfect reflector, i.e., $\epsilon = 0$. Determine the radiative heat flux between the disks if the channel wall is (*a*) specular, (*b*) diffuse. For simplicity, you may treat the channel wall as a single node. If the channel is made of a transparent material, the specular arrangement approximates the behavior of an optical fiber; if the channel is filled with air, the diffuse case approximates the behavior of a *light guide*, a device used to pipe daylight into interior, windowless spaces.

6.5 Two infinitely long parallel plates of width w are spaced $h = 2w$ apart. Surface 1 has $\epsilon_1 = 0.2$ and $T_1 = 1000\,\text{K}$, Surface 2 has $\epsilon_2 = 0.5$ and $T_2 = 2000\,\text{K}$. Calculate the heat transfer on these plates if (*a*) the surfaces are diffuse reflectors, (*b*) the surfaces are specular.

6.6 A long duct has the cross-section of an equilateral triangle with side lengths $L = 1\,\text{m}$. Surface 1 is a diffuse reflector to which an external heat flux at the rate of $Q_1' = 1\,\text{kW/m}$ length of duct is supplied. Surfaces 2 and 3 are isothermal at $T_2 = 1000\,\text{K}$ and $T_3 = 500\,\text{K}$, respectively, and are purely specular reflectors with $\epsilon_1 = \epsilon_2 = \epsilon_3 = 0.5$.

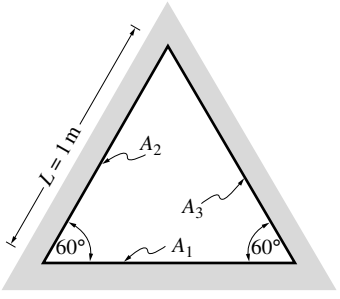

(*a*) Determine the average temperature of Surface 1, and the heat fluxes for Surfaces 2 and 3.

(*b*) How would the results change if Surfaces 2 and 3 were also diffusely reflecting?

6.7 Consider the infinite groove cavity shown. The entire surface of the groove is isothermal at T and coated with a gray, diffusely emitting material with emittance ϵ.

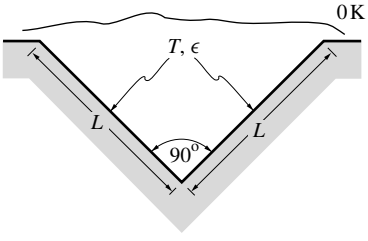

(*a*) Assuming the coating is a diffuse reflector, what is the total heat loss (per unit length) of the cavity?

(*b*) If the coating is a specular reflector, what is the total heat loss for the cavity?

6.8 Consider the infinite groove cavity shown in the adjacent sketch. The entire surface ($L = 2\,\text{cm}$) is isothermal at $T = 1000\,\text{K}$ and is coated with a gray material whose reflectance may be idealized to consist of purely diffuse and specular components such that $\epsilon = \rho^d = \rho^s = \frac{1}{3}$. What is the total heat loss from the cavity? What is its apparent emittance, defined by

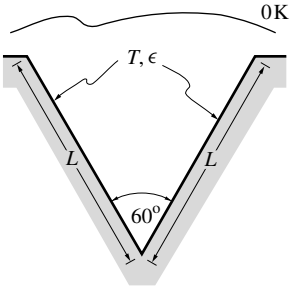

$$\epsilon_a = \frac{\text{total flux leaving cavity}}{\text{area of groove opening} \times E_b}\,?$$

6.9 Determine the temperature of surface A_2 in the axisymmetric configuration shown in the adjacent sketch, with the following data:

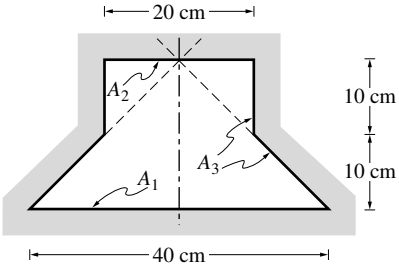

A_1 : $T_1 = 1000\,\text{K}$, $q_1 = -1\,\text{W/cm}^2$,
$\epsilon_1 = 0.6$ (diffuse reflector);

A_2 : $\epsilon_2 = 0.2$ (specular reflector);

A_3 : $q_3 = 0.0$ (perfectly insulated),
$\epsilon_3 = 0.3$ (diffuse reflector).

All surfaces are gray and emit diffusely.
Note: Some view factors may have to be approximated if integration is to be avoided.

6.10 To calculate the net heat loss from a part of a spacecraft, this part may be approximated by an infinitely long black plate at temperature $T_2 = 600\,\text{K}$, as shown. Parallel to this plate is an (infinitely long) thin shield that is gray and reflects specularly with the same emittance ϵ_1 on both sides. You may assume the surroundings to be black at 0 K. Calculate the net heat loss from the black plate.

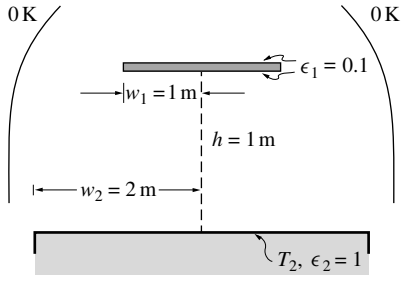

6.11 A long isothermal plate (at T_1) is a gray, diffuse emitter (ϵ_1) and purely specular reflector, and is used to reject heat into space. To regulate the heat flux the plate is shielded by another (black) plate, which is perfectly insulated as illustrated in the adjacent sketch. Give an expression for heat loss as a function of shield opening angle (neglect variations along plates). At what opening angle $0 \le \phi \le 180^\circ$ does maximum heat loss occur?

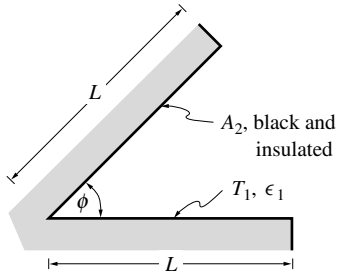

6.12 Reconsider Problem 6.11, but assume the entire configuration to be isothermal at temperature T, and covered with a partially diffuse, partially specular material, $\epsilon = 1 - \rho^s - \rho^d$. Determine an expression for the heat lost from the cavity.

6.13 An infinitely long cylinder with a gray, diffuse surface ($\epsilon_1 = 0.8$) at $T_1 = 2000\,\text{K}$ is situated with its axis parallel to an infinite plane with $\epsilon_2 = 0.2$ at $T_2 = 1000\,\text{K}$ in a vacuum environment with a background temperature of 0 K. The axis of the cylinder is two diameters from the plane. Specify the heat loss from the cylinder when the plate surface is (*a*) gray and diffuse, or (*b*) gray and specular.

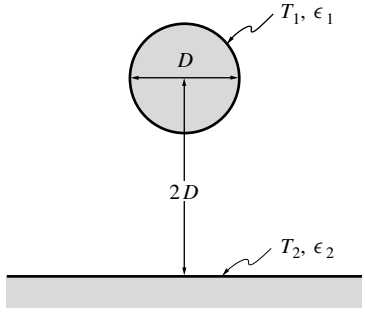

6.14 A pipe carrying hot combustion gases is in radiative contact with a thin plate as shown. Assuming *(a)* the pipe to be isothermal at 2000 K and black, *(b)* the thin plate to be coated on both sides with a gray, diffusely emitting/specularly reflecting material ($\epsilon = 0.1$), determine the radiative heat loss from the pipe. The surroundings are at 0 K and convection may be neglected.

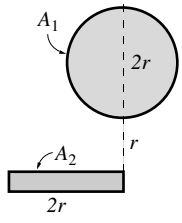

6.15 Repeat Problem 5.7 for the case that the flat part of the rod (A_1) is a purely specular reflector.

6.16 A long furnace may, in a simplified scenario, be considered to consist of a strip plate (the material to be heated, A_1: $\epsilon_1 = 0.2$, $T_1 = 500\,\text{K}$, specular reflector), unheated refractory brick (flat sides and bottom, A_2: $\epsilon_2 = 0.1$, diffuse reflector), and a cylindrical dome of heated refractory brick (A_3: $\epsilon_3 = 1$, $T_3 = 1000\,\text{K}$). Heat release inside the heated brick is q_h (W/m^2). The total heat release is radiated into the furnace cavity and is removed by convection, such that the convective heat loss is uniform everywhere (at q_c W/m^2 on all three surfaces).

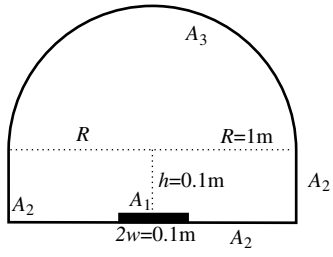

(a) Express the net radiative fluxes on all three surfaces in terms of q_h.
(b) Determine the q_h necessary to maintain the indicated temperatures.

6.17 A typical space radiator may have a shape as shown in the adjacent sketch, i.e., a small tube to which are attached a number of flat plate fins, spaced at equal angle intervals. Assume that the central tube is negligibly small, and that a fixed amount of specularly-reflecting fin material is available ($\epsilon = \rho^s = 0.5$), to give (per unit length of tube) a total, one-sided fin area of $A' = N \times L$. Also assume the whole structure to be isothermal. Develop an expression for the total heat loss from the radiator as a function of the number of fins (each fin having length $L = A'/N$). Does an optimum exist? Qualitatively discuss the more realistic case of supplying a fixed amount of heat to the bases of the fins (rather than assuming isothermal fins).

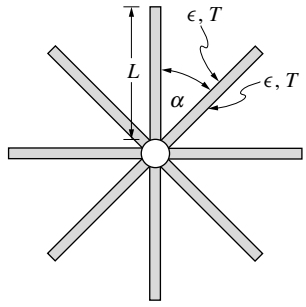

6.18 Repeat Problem 5.15 for the case that the stainless steel, while being a gray and diffuse emitter, is a purely specular reflector (all four surfaces).

6.19 Repeat Problem 5.16 for the case that both the platinum sphere as well as the aluminum shield, while being gray and diffuse emitters, are purely specular reflectors.

6.20 Repeat Problem 5.29, but assume steel and silver to be specular reflectors.

6.21 Reconsider the spacecraft of Problem 6.10. To decrease the heat loss from Surface 2 a specularly reflecting shield, of the same dimensions as the black surface and with emittance $\epsilon = 0.1$, is placed between the two plates. Determine the net heat loss from the black plate as a function of shield location. Where would you place the shield?

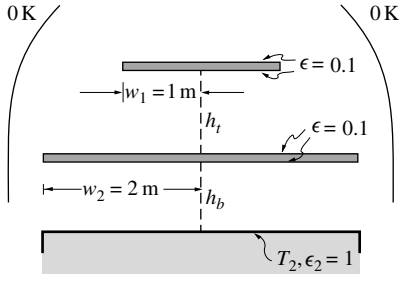

6.22 Evaluate the normal emittance for the V-corrugated surface shown in Fig. 6-10*a*. Hint: This is most easily calculated by determining the normal absorptance, or the net heat flux on a cold groove irradiated by parallel light from the normal direction; see Problem 6.8 for the definition of "apparent emittance."

6.23 Redo Problem 6.22 for an arbitrary off-normal direction $0 < \theta < \pi/2$ in a two-dimensional sense (i.e., determine the off-normal absorptance for parallel incoming light whose propagation vector is in the same plane as all the surface normal, namely the plane of the paper in Fig. 6-10).

6.24 A long, thin heating wire, radiating energy in the amount of $S' = 300\,\text{W/cm}$ (per cm length of wire), is located between two long, parallel plates as shown in the adjacent sketch. The bottom plate is insulated and specularly reflecting with $\epsilon_2 = 1 - \rho_2^s = 0.2$, while the top plate is isothermal at $T_1 = 300\,\text{K}$ and diffusely reflecting with $\epsilon_1 = 1 - \rho_1^d = 0.5$. Determine the net radiative heat flux on the top plate.

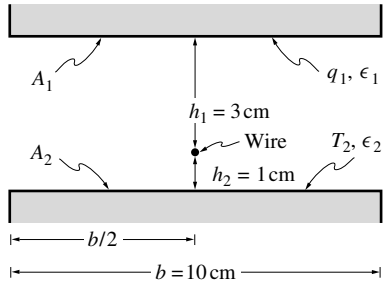

6.25 A long groove has diffuse walls that are insulated. All surfaces are gray with $\epsilon = 0.5$. A parallel beam of radiation, $q_0 = 1\,\text{W/cm}^2$ enters the open end of the cavity in the center line direction, flooding the cavity opening completely.

(*a*) What is the apparent reflectance of the groove (i.e., how much radiative energy is leaving it), and what is the temperature of surface A_1?

(*b*) What are these values if surface A_1 is a specular reflector instead of diffuse?

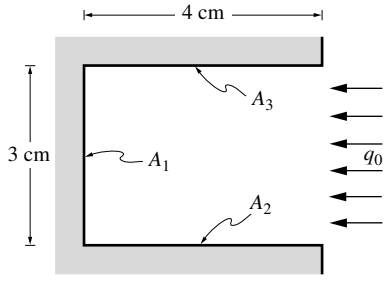

6.26 An infinitely long corner of characteristic length $w = 1\,\text{m}$ is a gray, diffuse emitter and purely specular reflector with $\epsilon = \rho^s = \frac{1}{2}$. The entire corner is kept at a constant temperature $T = 500\,\text{K}$, and is irradiated externally by a line source of strength $S' = 20\,\text{kW/m}$, located a distance w away from both sides of the corner, as shown in the sketch. What is the total heat flux Q' (per m length) to be supplied or extracted from the corner to keep the temperature at 500 K?

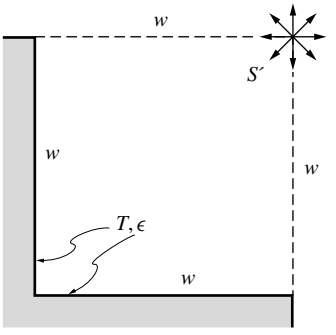

6.27 A long greenhouse has the cross-section of an equilateral triangle as shown. The side exposed to the sun consists of a thin sheet of glass (A_1) with reflectance $\rho_1 = 0.1$. The glass may be assumed perfectly transparent to solar radiation, and totally opaque to radiation emitted inside the greenhouse. The other side wall (A_2) is opaque with emittance $\epsilon_2 = 0.2$, while the floor (A_3) has $\epsilon_3 = 0.8$. Both walls (A_1 and A_2) are specular reflectors, while the floor reflects diffusely. For simplicity, you may assume surfaces A_1 and A_2 to be perfectly insulated, while the floor loses heat to the ground according to

$$q_{3,\text{conduction}} = U(T_3 - T_\infty)$$

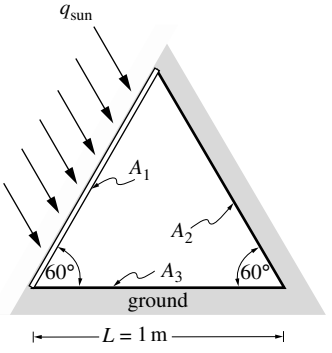

where $T_\infty = 280\,\text{K}$ is the temperature of the ground, and $U = 19.5\,\text{W/m}^2\,\text{K}$ is an overall heat transfer coefficient. Determine the temperatures of all three surfaces for the case that the sun shines onto the greenhouse with strength $q_{\text{sun}} = 1000\,\text{W/m}^2$ in a direction parallel to surface A_2.

6.28 Two long plates, parallel to each other and of width w, are spaced a distance $L = \sqrt{3}w/2$ apart, and are facing each other as shown. The bottom plate is a gray, diffuse emitter and specularly reflecting with emittance ϵ_1 and temperature T_1. The top plate is a gray, diffuse emitter and diffusely reflecting with emittance ϵ_2 and temperature T_2. The bottom plate is irradiated by the sun as shown (strength q_{sol} [W/m^2], angle θ). Determine the net heat fluxes on the two plates. How accurate do you expect your answer to be? What would be a first step to achieve better accuracy?

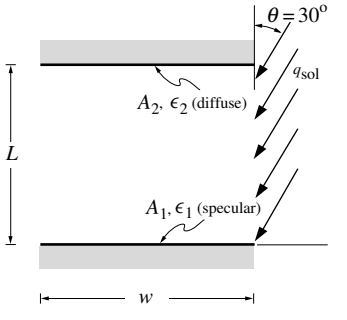

6.29 Consider the solar collector shown. The collector plate is gray and diffuse, while the insulated guard plates are gray and specularly reflecting. Sun strikes the cavity at an angle α ($\alpha < 45°$). How much heat is collected? Compare with a collector without guard plates. For what values of α is your theory valid?

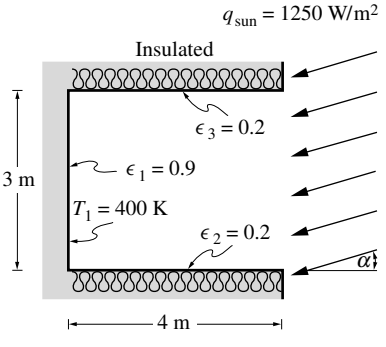

6.30 A rectangular cavity as shown is irradiated by a parallel-light source of strength $q_s = 1000\,\mathrm{W/m^2}$. The entire cavity is held at constant temperature $T = 300\,\mathrm{K}$ and is coated with a gray material whose reflectance may be idealized to consist of purely diffuse and specular components, such that $\epsilon = \rho^d = \rho^s = \frac{1}{3}$. How must the cavity be oriented toward the light source (i.e., what is ϕ?) so that there is no net heat flux on surface A_1?

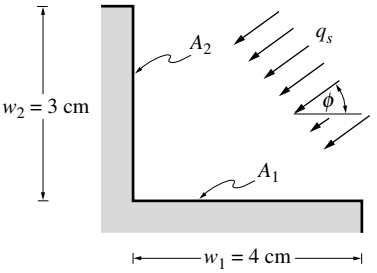

6.31 Reconsider the spacecraft of Problem 6.10. To decrease the heat loss from Surface 2 the specularly reflecting shield 1 is replaced by an array of N shields (parallel to each other and very closely spaced), of the same dimensions as the black surface and made of the original, specularly reflecting shield material with emittance $\epsilon = 0.1$. Determine the net heat loss from the black plate as a function of shield number N.

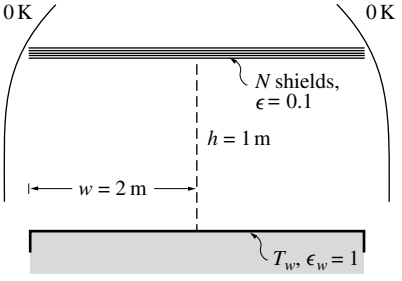

6.32 Repeat Problem 6.26 using subroutine `graydifspec` of Appendix F (or modifying the sample program `grspecxch`). Break up each surface into N subsurfaces of equal width ($n = 1, 2, 4, 8$).

6.33 Repeat Problem 6.24 using subroutine `graydifspec` of Appendix F (or modifying the sample program `grspecxch`). Break up each surface into N subsurfaces of equal width ($n = 1, 2, 4, 8$).

6.34 An infinitely long corner piece as shown is coated with a material of (diffuse and gray) emittance ϵ, and purely specular reflectance. Calculate the variation of heat flux along the surfaces per unit area. Both surfaces are isothermal at T_1 and T_2, respectively.

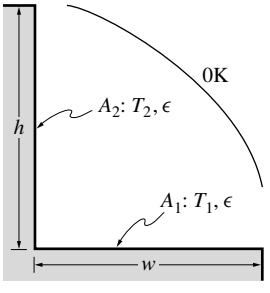

6.35 An infinitely long cavity as shown is coated with gray, specular materials ϵ_1 and ϵ_2 (but the materials are diffuse emitters). The vertical surface is insulated, while the horizontal surface is at constant temperature T_1. The surroundings may be assumed to be black at 0 K. Specify the variation of the temperature along the vertical plate.

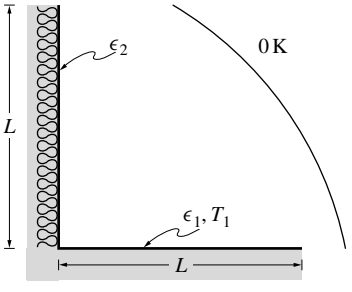

6.36 Consider the corner for Problem 6.30, which is irradiated by sunshine at an angle ϕ. Both plates are gray and specularly reflecting (emittance $\epsilon = 1 - \rho^s$) and isothermal at T. Develop an expression for the local heat fluxes as a function of ϵ, T, x, y, q_s, and ϕ.